DISCRIMINATING INTRA-PARASEQUENCE STRATIGRAPHIC UNITS FROM TWO-DIMENSIONAL QUANTITATIVE PARAMETERS

MANUEL F. ISLA, ERNESTO SCHWARZ, GONZALO D. VEIGA, JERÓNIMO J. ZUAZO, AND MARIANO N. REMIREZ

Centro de Investigaciones Geológicas, Universidad Nacional de La Plata–CONICET, Diagonal 113 #256, B1904DPK La Plata, Argentina
e-mail: misla@cig.museo.unlp.edu.ar

ABSTRACT: The intra-parasequence scale is still relatively unexplored territory in high-resolution sequence stratigraphy. The analysis of internal genetic units of parasequences has commonly been simplified to the definition of bedsets. Such simplification is insufficient to cover the complexity involved in the building of individual parasequences. Different types of intra-parasequence units have been previously identified and characterized in successive wave-dominated shoreface–shelf parasequences in the Lower Cretaceous Pilmatué Member of the Agrio Formation in central Neuquén Basin. Sedimentary and stratigraphic attributes such as the number of intra-parasequence units, their thickness, the proportions of facies associations in the regressive interval, the lateral extent of bounding surfaces, the degree of deepening recorded across these boundaries, and the type and lateral extent of associated transgressive deposits are quantitatively analyzed in this paper. Based on the analysis of these quantified attributes, three different scales of genetic units in parasequences are identified. 1) Bedset complexes are 10–40 m thick, basin to upper-shoreface successions, bounded by 5 to 16 km-long surfaces with a degree of deepening of one to three facies belts. These stratigraphic units represent the highest hierarchy of intra-parasequence stratigraphic units, and the vertical stacking of two or three of them typically forms an individual parasequence. 2) Bedsets are 2–20 m thick, offshore to upper-shoreface successions, bounded by up to 10 km long surfaces with a degree of deepening of zero to one facies belt. Two or three bedsets stack vertically build a bedset complex. 3) Sub-bedsets are 0.5–5 m thick, offshore transition to upper-shoreface successions, bounded by 0.5 to 2 km long surfaces with a degree of deepening of zero to one facies belt. Two or three sub-bedsets commonly stack to form bedsets. The proposed methodology indicates that the combination of thickness with the proportion of facies associations in the regressive interval of stratigraphic units can be used to discriminate between bedsets and sub-bedsets, whereas for higher ranks (bedsets and bedset complexes) the degree of deepening, lateral extent of bounding surfaces, and the characteristics of associated shell-bed deposits become more effective. Finally, the results for the Pilmatué Member are compared with other ancient and Holocene examples to improve understanding of the high-frequency evolution of wave-dominated shoreface–shelf systems.

INTRODUCTION

High-resolution sequence stratigraphy typically deals with subseismic-scale analyses (fourth-order and lower ranks), focusing particularly on parasequences and intra-parasequence stratigraphic units (Van Wagoner et al. 1988, 1990; Mitchum and Van Wagoner 1991; Kamola and Van Wagoner 1995; Posamentier and Allen 1999). Many high-resolution hierarchical analyses of such units are restricted by the current definition of parasequences, the constituent units of which are referred to simply as bedsets (e.g., O'Byrne and Flint 1995). However, one of the main problems with analyzing the high-frequency stratigraphic record of shallow-marine parasequences (PSs) is the variability of criteria that can be considered. The overlapping scale and rather similar definitions of parasequences and bedsets have led to some confusion that sequence stratigraphers have tried systematically to solve (Hampson 2000; Zecchin et al. 2017; Schwarz et al. 2018; Ainsworth et al. 2019). Bedsets have traditionally been defined as "concordant successions of genetically related beds within parasequences, limited by surfaces of non-deposition or erosion, and their correlative conformities" (*sensu* Van Wagoner et al. 1990). This concept derived from the original definition of bedsets being sets of strata (Campbell 1967). In this sense, the bedset definition of Van Wagoner et al. (1990) presents a problem for sequence-stratigraphy practitioners because it does not imply any specific scale, apart from bedsets being smaller units contained within parasequences. Recently, Catuneanu (2019) indicated that relatively conformable successions can be defined at every stratigraphic scale, but the difference among them lies in the scale of their bounding unconformities. Thus, the term bedset is commonly used to denote a wide range of different high-frequency stratigraphic units recognized in ancient shoreface–shelf parasequences. There have been some efforts to expand this two-fold hierarchy (i.e., parasequences and bedsets) into a general intra-parasequence genetic architectural scheme (Ainsworth et al. 2017, 2019), but the resulting schemes appear to be so complex that they may not be easy to apply, particularly in non-deltaic successions.

The application of the two-fold hierarchy has led to inconsistencies when stratigraphic units defined as bedsets in different studies are compared in terms of bounding surfaces, thicknesses, and time duration.

This discrepancy increases when intra-parasequence analysis is applied to the well-constrained and well-dated Holocene stratigraphic record, which still represents a less explored period for sequence stratigraphy. Recently, high-resolution analysis and the definition of parasequences in Holocene strandplain successions has been used to understand the impact of factors (such as sea-level fluctuations) controlling and influencing the resulting sedimentary record of shallow-marine systems (Amorosi et al. 2008, 2017; Bruno et al 2017; Berton et al 2018). The Holocene sedimentary record is thus becoming an excellent framework for comparing depositional units with the intra-parasequence stratigraphy of ancient depositional systems. In this context, several studies have proposed different equivalences between high-frequency genetic units in both ancient and recent depositional systems (Hampson et al. 2008; Sømme et al. 2008; Ainsworth et al. 2019). However, to facilitate such comparative approaches, it is necessary to clarify the criteria used to define stratigraphic units (Catuneanu 2019). The accurate definition of intra-parasequence genetic units in shoreline environments requires the analysis of the prograding shoreface–shelf profile, as well as the stratigraphic discontinuities generated by relative sea-level changes (Hampson 2000; Hampson and Storms 2003; Sømme et al. 2008; Isla et al. 2018). Several stratigraphic attributes inherent to both aspects, and commonly used for the definition of high-frequency genetic units, need to be re-evaluated (thickness, facies proportions, extent of discontinuities, degree of deepening across bounding surfaces), to establish a unified set of diagnostic criteria.

Thus, to evaluate key sedimentological and stratigraphical criteria to identify intra-parasequence units and their hierarchical relationships, this study focuses on shallow-marine parasequences of the Lower Cretaceous Pilmatué Member occurring in the Neuquén Basin (Argentina). A well-exposed 25-km proximal–distal transect and of this well-dated unit offers an excellent opportunity to study the intra-parasequence architecture and hierarchy of depositional units at various scales, in a stacked succession of parasequences. Particularly, the sand-rich, upper half of the Pilmatué Member allows the lateral tracing of parasequences and intra-parasequence units, and a systematic quantitative analysis of several attributes such as (but not limited to): thickness variations, facies proportions, lateral extent of bounding surfaces, and the stratigraphic distribution of transgressive deposits. The combination of these quantified parameters provides a more robust sequence-stratigraphic scheme for the studied interval and proves that the previously defined bedsets in the Pilmatué Member can be assigned to at least three different orders of genetic unit. Thus, the first objective of this paper is to establish a consistent high-resolution sequence-stratigraphic framework for the intra-parasequence architecture of the upper half of the Pilmatué Member, which expands the hierarchy of genetic units in these strata beyond parasequences and bedsets. The second objective of this paper is to use the high-resolution hierarchy for the Pilmatué Member to establish a set of diagnostic criteria for recognizing and defining the wide range of intra-parasequence units that may occur in shoreface–shelf parasequences worldwide. The resulting intra-parasequence architecture is then discussed in relation to other high-resolution analyses from the ancient and Holocene sedimentary record, particularly comparing the proposed sedimentary and stratigraphic criteria for intra-parasequence genetic units. The incorporation of a consistent and robust methodology for the definition of high-resolution genetic units will allow researchers to standardize learnings from both ancient and recent shallow-marine successions worldwide.

GEOLOGICAL SETTING AND STUDY AREA

The Neuquén Basin is located in west-central Argentina between 32° and 40° S latitude and it is bounded by the Andean Volcanic Arc to the west, the Sierra Pintada System to the northeast, and the North Patagonian Massif to the southeast (Fig. 1A). The Neuquén Basin is characterized by a complex tectono-stratigraphic evolution through the Late Triassic to the early Cenozoic, commonly considered to constitute three main stages: 1) syn-rift phase, 2) post-rift phase, and 3) foreland phase (Howell et al. 2005). During the Early to Middle Jurassic, rifting ceased, and the basin developed into a back-arc basin. During this post-rift period (which include the period of accumulation of the studied succession), through the Late Jurassic and into the Early Cretaceous, eustatic changes combined with recurrent uplift of the magmatic arc conditioned the connection between the proto–Pacific Ocean and the semi-enclosed marine basin (Legarreta and Uliana 1991).

The Pilmatué Member constitutes the lowermost unit of the Agrio Formation, which accumulated during the late Valanginian and early Hauterivian (Fig. 1B). The Pilmatué Member overlies the Mulichinco Formation in the western sector, which includes continental, marginal-marine, and marine facies (Schwarz and Howell 2005; Schwarz et al. 2006) and is covered by continental deposits of the Avilé Member (Veiga et al. 2007). The base of the Pilmatué Member marks a sudden deepening of the basin (Legarreta and Uliana 1991; Schwarz et al. 2006), and the development of a low-gradient marine ramp environment in a back-arc setting. This unit is up to 650 m thick and consists predominantly of marine shales and marls, which record deposition under offshore, basinal conditions. Subordinate sandstone packages are intercalated with the fine-grained deposits, recording the repeated progradation of a wave-dominated shoreface–shelf system (Spalletti et al. 2011; Schwarz et al. 2018). Deltaic systems have been reported to occur locally in the central part of the basin (Schwarz et al. 2021). Whereas most of the basin-fill succession is siliciclastic, the presence of carbonates is significant, either forming fine-grained basinal intervals of almost pure carbonate in the north (Remirez et al. 2020; Moore et al. 2020), as well as mixed carbonate–siliciclastic shoreface deposits with skeletal and ooid contributions (Schwarz et al. 2018).

The study area, near the town of Chos Malal (Fig. 1C), is located at the eastern margin of the Agrio Fold and Thrust Belt, which is a large structural belt of thin-skinned structures (Zamora Valcarce et al. 2007). A late Miocene compressional event marked the final shaping of this morphostructure, generating several north- to south-oriented fold and thrust belts. Here the Pilmatué Member crops out along the flanks of three anticlines that collectively form a continuous, accessible, and poorly vegetated outcrop, ca. 25 km long and up to 8 km wide (Fig. 1C). Only in the northernmost 4 km of the studied outcrop transect is the stratigraphic section not fully exposed. In the study area, the investigated succession is up to 300 m thick, conforms to the upper interval of the Pilmatué Member (Remirez et al. 2020), and is composed of fine-grained lithologies (gray shales and marls, greenish mudstones, and sandy mudstones) in its lower half, and fine-grained deposits interbedded with coarsening-upward, decameter-thick intervals comprising muddy sandstones, fine-grained sandstones, mixed sandstone–carbonate deposits, and skeletal carbonates in its the upper half (Schwarz et al. 2018). North of the study area (central and northern part of Curaco anticline; Fig. 1C), the sandstone packages are almost absent (Remirez et al. 2020), suggesting a general northward fining, and hence more distal conditions, in that direction (Schwarz et al. 2018).

Previous Work on Facies Associations and Parasequence Definition in the Investigated Succession

Across the study area, the Pilmatué Member can be subdivided into two stratigraphic intervals (Fig. 1B). The lower half is of late Valanginian age and is largely dominated by mudstones and marls deposited in the distal, basinal segments of a mixed siliciclastic–carbonate marine system (Remirez et al. 2020). Parasequences are not clearly defined in this lower interval (Schwarz et al. 2018) and therefore are not analyzed in this paper.

The upper half of the Pilmatué Member, of early Hauterivian age (Schwarz et al. 2016a), has been widely studied at different scales and/or locations by several contributions (Isla et al. 2018, 2020a, 2020b, 2020c;
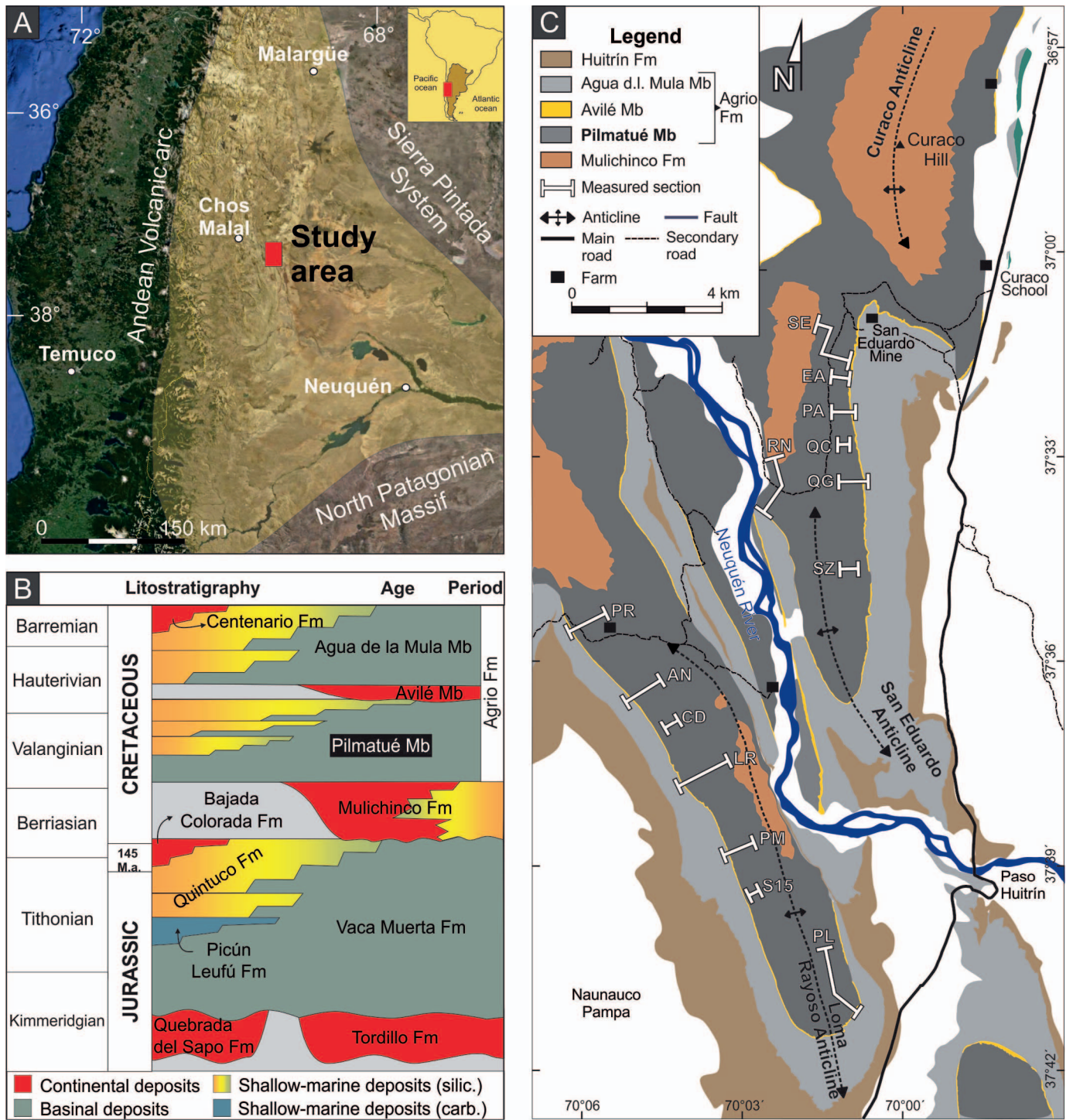
FIG. 1.—**A)** Location of the study area in the Neuquén Basin. The extent of the basin is outlined in yellow. **B)** Chronostratigraphic chart of the Upper Jurassic to Lower Cretaceous Mendoza Group, culminating in the Valanginian–Barremian Agrio Formation. The Pilmatué Member, which is the focus of this study, represents the lower unit of the Agrio Formation. **C)** Geological map of the study area showing the main exposures of the Pilmatué Member. The location of the 14 sedimentary sections investigated in this study are indicated. These are the investigated sections: PL, Puesto Ladrillo; S15, South 15; PM, Puesto Mardone; LR, Loma Rayoso; CD, Cóndores; AN, Anfiteatro; PR, Puesto Riquelme; SZ, Solorza; RN, Río Neuquén; QG, Quebrada Grande; QC, Quebrada Chica; PA, Puesto Abandonado; EA, El Abra; SE, San Eduardo (modified from Schwarz et al. 2018).

TABLE 1.—*Facies associations chart.*

Facies Associations	Lithology	Sedimentary Structures; Thickness	Traces Fossils; Fossils	Interpretation
Basin (BA)	Siliciclastic and carbonate shale	Fissility, uncommon structureless; up to 95 m	Typically barren (BI 0–1); ammonites, foraminifera, radiolarians	Settling from suspension on a low-energy, poorly oxygenated sea floor. Mixed (carbonate–siliciclastic) basinal setting
Offshore (OF)	Mudstones grading to siltstones	Planar-bedded lamination or massive; < 35 m	*Thalassinoides*, *Chondrites* (BI 5–6); *Cucullaea* sp., *Eriphyla* sp., *Steimanella* sp	Settling from suspension on a low-energy, well-oxygenated sea floor
Offshore transition (OT)	Intercalated mudstones and siltstones with sand discrete beds. Subordinate muddy sandstones	Dominant lenticular and wavy bedding with cross-lamination and symmetrical ripples, subordinate hummocky cross-stratification; < 9 m	*Palaeophycus*, *Thalassinoides*, *Teichichnus*, *Planolites*, *Asterosoma*, *Rosselia*, *Ophiomorpha*, *Gyrochortes* (mud-dominated: BI 5–6; sand-dominated: BI 3–4); *Panopea* sp., *Eriphyla* sp., *Steimanella* sp., *Pinna* sp.	Alternation of settling from suspension and sandy distal storm events, below fair-weather wave base and above storm wave base. Transition zone from offshore to shoreface
Lower shoreface (LS)	Very fine to fine-grained sandstones	Amalgamated HCS beds. Ripple-cross lamination and symmetrical to lightly asymmetrical ripples; < 9 m	*Ophiomorpha*, *Skolithos*, *Palaeophycus*, *Arenicolites*, *Gyrochortes*, *Rosselia* (BI 1–6); rare *Steimanella* sp.	Large asymmetrical ripples and hummocks by oscillatory and combined storm-related flows, Wave-induced fair-weather conditions. Storm-dominated, wave-influenced lower shoreface
Upper shoreface (US)	Siliciclastic and mixed fine-grained and pebbly sandstones	Planar and trough cross-stratification; < 5 m	*Ophiomorpha*, *Arenicolites* (BI 0–2); undetermined bivalves, oysters	Dune migration under unidirectional currents. Upper shoreface conditions in a bar-trough morphology
Shoreface shell beds (SSB)	Pebbly mixed sandstones (gravel-size bioclasts and ooids, sandstone clasts)	Trough cross-lamination. Asymmetrical ripples–dunes; < 0.5 m	Absent; *Ceratostreon* sp., *Pholadomya* sp., *Ptychomya* sp., *Steimanella* sp., *Trigonia* sp., echinoids, gastropods	Reworking near or below fair-weather wave base by wave action and storm-related flows. Shoreface during transgressive conditions
Offshore shell beds (OSB)	Skeletal-dominated, mixed floatstone, dominant gravel-size bioclasts, less sand-size bioclasts, terrigenous silt and ooids	Massive; commonly < 0.5 m thick, rarely up to 15 m	Absent; *Ceratostreon* sp., *Parsimonia* sp., *Columastrea* sp., *Eriphyla* sp., *Cucullaea* sp., *Panopea* sp., *Ptychomya* sp., *Pholadomya* sp., *Steimanella* sp., *Aetostreon* sp., pectinids, ammonites	Reduced physical reworking. Basinal, Offshore and Offshore-transition settings during transgressive conditions

Schwarz et al. 2018; Remirez et al. 2020) and is the focus of the present study. Schwarz et al. (2018) characterized this upper interval as a mixed, siliciclastic-dominated shoreface–shelf system. The identification of facies associations representing the progradation and retrogradation of this shoreface–shelf depositional system is fundamental to subdivide parasequences into IPUs and to generate much of the quantitative data used for the present contribution.

Seven facies associations (Table 1) have been recognized in the study interval (Spalletti et al. 2011; Isla et al. 2018; Schwarz et al. 2018; Remirez et al. 2020) and attributed to specific segments of a mixed (carbonate–siliciclastic), shoreface–shelf depositional setting: basin (BA), offshore (OF), offshore transition (OT), lower shoreface (LS), upper shoreface (US), shoreface shell bed (SSB) and offshore shell bed (OSB) facies associations. The first five associations were interpreted as representing the progradation of a storm-dominated shoreface–shelf system. The last two (SSB and OSB) were directly linked to the development of transgressive surfaces and represent retrogradational conditions.

Basin deposits (BA) are composed of fissile, dark gray to black shale, in which even fissility is ubiquitous but a structureless appearance is observed locally. This facies association is overlain by offshore deposits (OF) comprising coarsening-upward intervals with massive, siliciclastic mudstone at the base that grades upward to structureless siltstone. Overlying offshore facies, heterolithic deposits consisting of muddy sandstones and subordinate hummocky cross-stratified sandstones represent the offshore-transition facies association (OT). Heterolithic deposits are mostly

composed of siltstone interbedded with lenticular, cross-laminated sandstones. The shallowing-upward succession continues with the lower-shoreface (LS) facies association represented by amalgamated sandstone beds having variable physical sedimentary structures, as well as intensely bioturbated sandy packages (Table 1). Beds of very fine-grained sandstone with hummocky cross-stratification are dominant, whereas planar-bedded lamination, low-angle lamination or swaly cross-stratification may occur. Finally, upper-shoreface deposits (US) consisting of fine-grained, cross-stratified, siliciclastic sandstones and mixed carbonate–siliciclastic sandstones cap the regressive interval (Table 1). Mixed carbonate–siliciclastic sandstone commonly occurs as subordinate lenses in the siliciclastic sandstone, typically in the lower part of the troughs of cross-bed sets. However, mixed carbonate–siliciclastic sandstone also exists as discrete intervals up to 2 m thick of better-sorted sand-size material that is mostly composed of ooids, bioclasts, and terrigenous grains. Paleocurrents from trough axes show a predominant northward to eastward direction (mean to the northeast). Current ripples are commonly associated with cross-bedded sets.

The vertical (and lateral) stacking of the facies associations define a regressive interval resulting from the progradation of a shoreface–shelf system. This depositional system transitions from low-energy, poorly oxygenated, mixed (siliciclastic–carbonate) basinal and offshore settings located well below storm-wave base to shallower areas with an increasing influence of waves and currents (Isla et al. 2018; Schwarz et al. 2018; Remirez et al. 2020). In the offshore transition there was an alternation

between processes of settling from suspension during fair-weather conditions (mud deposition) and accumulation of sands transported by oscillatory and combined flows generated during storm events. Most of the silt and very fine sand, however, was later mixed with mud due to intense bioturbation. This storm-dominated offshore–shoreface transition was located between storm-wave base and fair-weather wave base. Above the fair-weather wave base, the lower-shoreface setting was constantly subjected to wave action, where sand was mostly transported and deposited by storm-related flows and fair-weather waves (Isla et al. 2018, 2020a; Schwarz et al. 2018). Finally, the upper-shoreface setting reflects the development of relatively permanent unidirectional currents that formed subaqueous dunes. These bedforms were produced in troughs and/or rip channels (Isla et al. 2020a, 2020b). Low bioturbation intensity suggests unstable and highly energetic substrates, and abundant bioclasts and ooids suggest fairly continuous mixing of in situ-produced carbonates together with siliciclastic grains.

Shallowing-upward packages are frequently interrupted by coarser-grained, mixed (siliciclastic–carbonate) deposits that are collectively referred to as shell beds. The shoreface shell bed facies association (SSB) is characterized by discontinuous, erosionally based, thin beds composed of pebbly and skeletal sandstones (Table 1). These thin conglomerates can be massive or exhibit trough cross-stratification with 3D symmetric dunes preserved on the bed top. This facies association has been interpreted to be the result of reworking processes in shoreface settings by wave and current action during transgressions (Isla et al. 2018; Schwarz et al. 2018). The other transgressive facies association is denoted as offshore shell beds (OSB), and consist of skeletal-dominated, mixed (carbonate–siliciclastic) facies (Table 1; Schwarz et al. 2018). These mixed deposits have a limestone- and mudstone-dominated matrix and skeletal fragments commonly corresponding to epibenthic or endobenthic bivalves, but corals, serpulids, and ammonoids may also be present. Fossils commonly exhibit a high degree of articulation and erosion, whereas fragmentation is relatively low. The OSB was interpreted as representing maximum condensation in offshore settings during transgressions (Schwarz et al. 2018).

In the studied interval, shallow-marine wedges, formed by the seven facies associations described above (Table 1), comprise multiple shallowing-upward successions conforming to parasequences (Schwarz et al. 2018) (Fig. 2). The parasequences described in this study could be better defined as high-frequency sequences because they include transgressive deposits (Zecchin and Catuneanu 2013), but for simplicity they will be termed as parasequences herein. Schwarz et al. (2018) systematically defined parasequences as those intervals bounded by transgressive surfaces exhibiting at least a vertical shift (i.e., abrupt upward deepening of facies) of two facies belts in any sector of the study area (e.g., basin deposits overlying offshore-transition deposits and/or offshore deposits on top of lower-shoreface deposits). In this way, Schwarz et al. (2018) documented the presence of 17 parasequences (numbered from base to top) in the upper half of the Pilmatué Member, each characterized by shallowing-upward, shoreface–offshore packages (30–50 m thick), bounded by extensive transgressive surfaces.

METHODS

This paper builds on the outcrop correlation and interpretation of the upper half of the Pilmatué Member in a 25-km-long proximal–distal transect presented by Schwarz et al. (2018) for 17 parasequences (Fig. 2), as well as by detailed correlation and interpretation presented by Isla et al. (2018) for one single parasequence in the uppermost section of the study interval (Fig. 3). This north-to-south correlation panel covering the upper half of the Pilmatué Member was built from a total of 14 sedimentary logs, which are typically located less than 2 km apart (Figs. 1C, 2). Most of the logs document the entire upper half of the Pilmatué Member. Standard

sedimentological data (texture, sedimentary structures, paleocurrents, and thickness) were combined with ichnofaunal, macrofaunal, and taphonomic data (bioturbation intensity, degree of articulation, degree of fragmentation, etc.) to define and interpret facies and facies associations in the original contribution (Schwarz et al. 2018). Key stratigraphic surfaces (mostly transgressive surfaces) were walked out and mapped laterally in the field. Most of these surfaces could be traced from sand-prone to mud-rich intervals in the field, because many transgressive surfaces in mudstone-dominated offshore intervals are demarcated by shell beds (Figs. 2, 3). More extensive correlations were also aided by high-resolution aerial photographs of the excellent exposures. Only in the northernmost basinal-dominated sectors of the transect are the individual parasequences hard to define (e.g., Fig. 3C, PS260 to PS280). The upper section of the correlation panel (Fig. 2C) represents data collected with a higher degree of resolution by Isla et al. (2018), in which more than 25 sedimentary logs, separated by less than 500 m, were used. For practical reasons, not all these logs have been used for the quantitative analysis.

For the quantitative analyses presented in this contribution only 10 of the 17 previously identified parasequences have been selected: PS260, PS270, PS280, PS290, PS300, PS340, PS350, PS360, PS380, and PS400 (Fig. 2), because their intra-parasequence units achieved the needs for the desired quantification. To avoid overlap with previous terminology, all genetic units defined in these 10 parasequences will be referred as intra-parasequence units (IPUs) in the present study (Table 2). These IPUs are here defined, in a similar way to bedsets, as relative conformable successions bounded by stratigraphic surfaces in parasequences. The current numbering of these units (Table 2) is directly related to their stratigraphic position in the well-established parasequence framework of Schwarz et al. (2018) (e.g., IPU360.1 represents the basal, older IPU of parasequence PS360 and IPU360.2 would be the overlying, younger one, Fig. 2A).

Sedimentologic and Stratigraphic Attributes of IPUs

Sedimentologic and stratigraphic attributes in this contribution were quantified and combined to objectively characterize the intra-para-sequence units and their bounding surfaces. The attributes considered here include: 1) the number of IPUs within a parasequence, 2) the thickness of IPUs, 3) the facies proportions in the regressive interval of each IPU, 4) the degree of deepening across the bounding surfaces of the IPUs, 5) the lateral extent of surfaces bounding the IPUs and, 6) the type and lateral extent of the thin transgressive deposits. These sedimentary and stratigraphic attributes change vertically in each measured section, as well as between sections, recording deposition in the proximal setting (in the southern part of the study area) and those representing deposition mostly in distal settings (in the northern part of the study area). Therefore, the analysis includes investigations of both the vertical and lateral relationships. In this way, estimated attributes are representative of the depositional settings and processes operating during the deposition of each genetic unit at a given location. Occasionally parasequences are discriminated between sandstone-dominated (sandstone facies constitute more than the 40% of the total thickness) and mudstone-dominated parasequences (sandstone facies constitute less than the 40% of the total thickness). Based on the previous analysis, the shallowing-upward succession of basin, offshore, offshore-transition, lower-shoreface, and upper-shoreface facies associations are interpreted as representing regressive conditions, whereas the presence of shoreface shell beds and offshore shell beds correspond to deepening-upward intervals represent-ing transgressive conditions. Besides, the degree of deepening is analyzed by considering the vertically upward facies change between the top of the underlying and the base of the overlying regressive interval (excluding transgressive shell beds from the analysis).
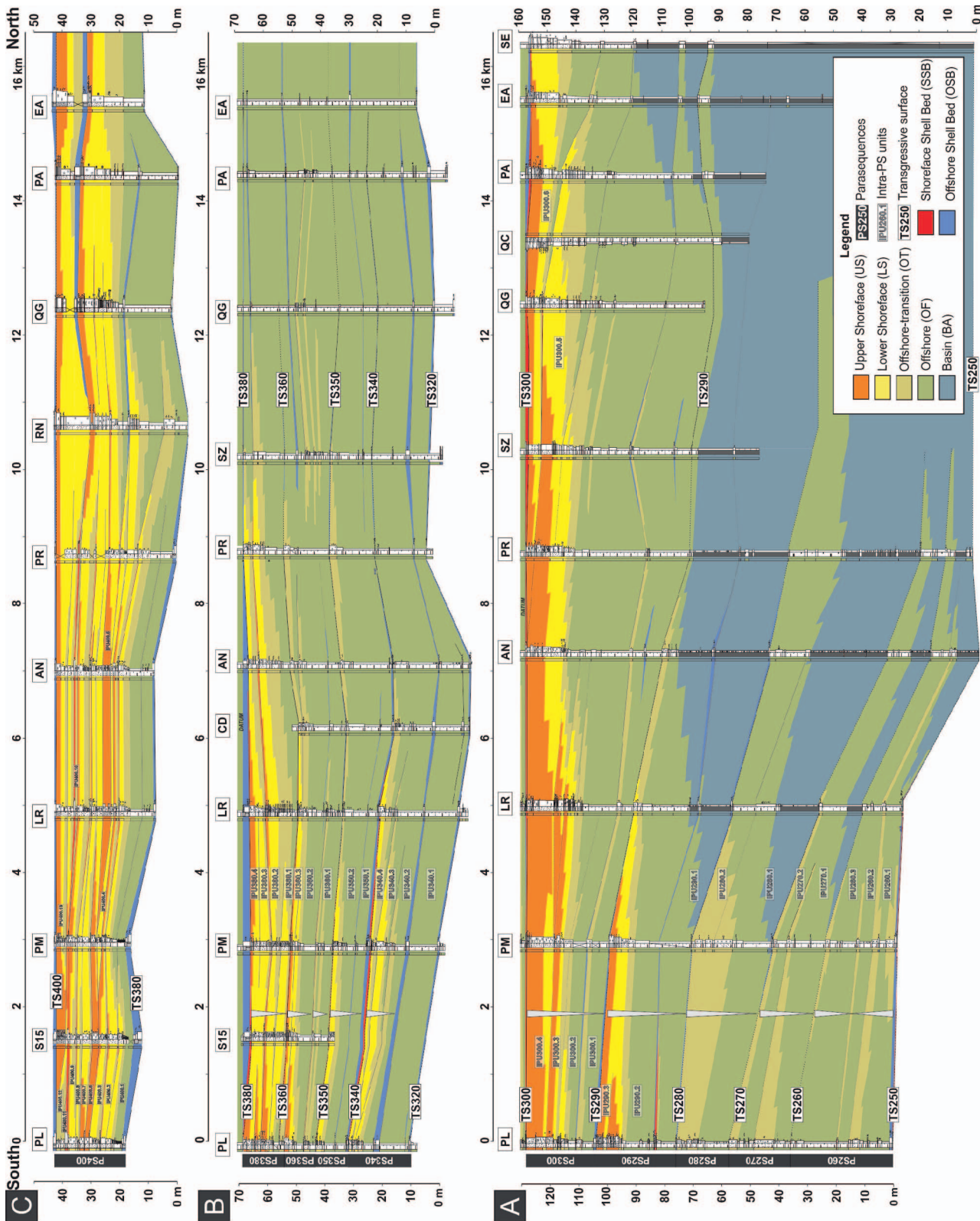
Fig. 2.—The three north–south-oriented correlation panels (approximately along depositional dip), used for the intra-parasequence architectural analysis. Ten parasequences from the upper half of the Pilmatué Member were studied. Depositional architecture and facies distribution of parasequences: **A)** PS260 to PS300, **B)** PS340 to PS380, **C)** PS400; compiled from Isla et al. (2018) and Schwarz et al. (2018). Flattening datums: A) TS300, B) TS380, C) TS400.
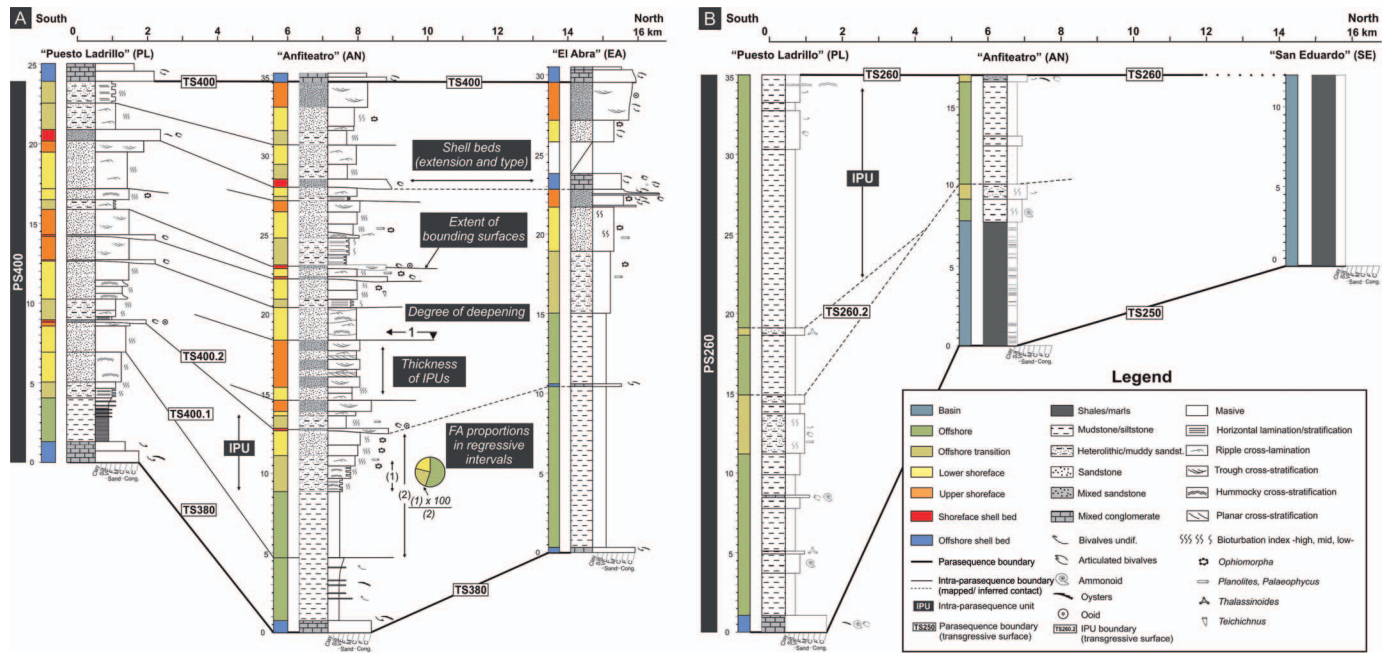
Fig. 3.—Examples of detailed sedimentary logs used for facies analysis and the correlation of key stratigraphic surfaces. The main sedimentary and stratigraphic attributes used for the quantitative analyses are also illustrated. **A)** Selected sections from PS400 recording a proximal development with abundant upper-shoreface deposits. The complete parasequence architecture is shown in Figure 2A. **B)** Selected sections from PS260, which record a distal development dominated by offshore-transition to basinal facies. The correlation panel is flattened on the TS260. The complete parasequence architecture is shown in Figure 2C.

TABLE 2.—*Previous sequence-stratigraphic terminology used for the Pilmatué Member.*

Genetic Units and Stratigraphic Surfaces	Nomenclature	Stratigraphy of the Pilmatué Member (from base to top)	Description
Bedset or intra-parasequence unit	B/IPU	IPU260.1, IPU260.2, IPU260.3, IPU270.1, IPU270.2, IPU280.1, IPU280.2, IPU290.1, IPU290.2, IPU290.3, IPU300.1, IPU300.2, IPU300.3, IPU300.4, IPU300.5, IPU300.6, IPU340.1, IPU340.2, IPU340.3, IPU340.4, IPU350.1, IPU350.2, IPU360.1, IPU360.2, IPU360.3, IPU380.1, IPU380.2, IPU380.3, IPU380.4, IPU400.1, IPU400.2, IPU400.3, IPU400.4, IPU400.5, IPU400.6, IPU400.7, IPU400.8, IPU400.9, IPU400.10, IPU400.11, IPU400.12, IPU400.13	Concordant successions of genetically related beds in parasequences, constituting shallowing-upward packages limited by surfaces of nondeposition or erosion, and their correlative conformities (Van Wagoner et al. 1990).
Parasequence	PS	PS260, PS270, PS280, PS290, PS300, PS340, PS350, PS360, PS380, PS400	Concordant successions of genetically related beds, constituting shallowing-upward packages bounded by stratigraphic surfaces that represent abrupt marine flooding (Van Wagoner et al. 1988). Also, high-frequency sequences (Zecchin and Catuneanu 2013).
Bedset or IPU boundary	e.g., TS260.1	TS260.1, TS260.2, TS270.1, TS280.1, TS290.1, TS290.2, TS300.1, TS300.2, TS300.3, TS300.4, TS300.5, TS340.1, TS340.2, TS340.3, TS350.1, TS360.1, TS360.2, TS380.1, TS380.2, TS380.3, TS380.4, TS400.1, TS400.2, TS400.3, TS400.4, TS400.5, TS400.6, TS400.7, TS400.8, TS400.9, TS400.10, TS400.11, TS400.12	Bounding surfaces between successive bedsets or IPUs.
Parasequence boundary	e.g., TS260	TS250, TS260, TS270, TS280, TS290, TS300, TS320, TS340, TS350, TS360, TS380, TS400	Bounding surfaces between successive parasequences.
Transgressive surface	TS	*NA*	Stratigraphic surface of erosion or nondeposition generated during the landward migration of the shoreline.
Wave-ravinement surface	WRS	*NA*	Surface of erosion (Hampson 2000), generated by wave action during the landward migration of the shoreline.
Non-depositional surface	ND	*NA*	Surface of nondeposition (Hampson 2000) generated by sediment starvation during the landward migration of the shoreline.

Number of IPUs within a Parasequence.—The number of IPUs is scale-independent and consists of the sum of internal units that can be identified within each parasequence.

Thickness of IPUs.—The thickness was measured between successive bounding surfaces, and hence considers both transgressive and regressive intervals (Fig. 3). Transgressive deposits are typically thin, constituting up to 15% of total parasequence thickness.

Facies Proportion in the Regressive Interval of Each IPU.—In any small-scale transgressive–regressive unit, the regressive package or hemicycle is defined as the stratigraphic interval in which the vertical stacking of successive facies associations suggests the progradation of the shoreface–shelf profile, whereas the transgressive interval is represented by the shell bed facies associations, either as one single thin deposit or a deepening-upward succession with both shell-bed types (Schwarz et al. 2018). We define for this study the facies proportion in the regressive interval of each IPU as the percentage of basin, offshore, offshore-transition, lower-shoreface, and upper-shoreface facies associations compared to the total thickness of the same regressive interval. These percentage values (referred as percentage values of parasequence thickness), were plotted in pie charts together with their stratigraphic position and associated bounding surfaces (see Fig. 3A for an example in the Anfiteatro section).

The Degree of Deepening across the IPU Bounding Surfaces.—The degree of deepening (DD) is a measurement of the flooding across the surface and is here defined as the number of facies belts that are shifted across a transgressive surface (Fig. 3). Considering that in the proposed shoreface-to-basinal depositional model five facies belts were defined, DD4 represents the maximum possible flooding when upper-shoreface deposits are overlain by basinal mudstones, whereas the minimum deepening degree represents the same facies belt across the boundary (DD0).

The Lateral Extent of IPU Bounding Surfaces.—This parameter is directly related to the elongation of the stratigraphic expression (vertical change of facies) across IPU bounding surfaces along the proximal-to-distal profile. Considering that the investigated outcrop belt is oriented subparallel to the depositional dip (Fig. 2), these measurements represent the down-dip extent of the bounding surfaces across the depositional system. Transgressive surfaces (i.e., fourth- to sixth-order surfaces) are commonly well defined near the shoreline and become more cryptic both seaward and landward (Cattaneo and Steel 2003). It is expected that the higher the degree of deepening defined in proximal settings, the larger the mappable extent of the surface.

The Type and Lateral Extent of Thin Transgressive Deposits.—This parameter focuses on the analysis of the thin transgressive deposits demarcating parasequence and IPU bounding surfaces (SSB and OSB facies associations; Table 1). The occurrence, type, and vertical and lateral transition of shell-bed deposits are evaluated. The vertical and lateral distribution across the study area typically depend on the facies below and above, and the degree of deepening.

QUANTITATIVE ANALYSES OF THE INTRA-PARASEQUENCE SEDIMENTARY AND STRATIGRAPHIC ATTRIBUTES IN THE STUDY AREA

Number of IPUs within a Parasequence

Based on the vertical and lateral distribution of facies associations, 42 intra-parasequence units (IPUs) were recognized within the 10 investigated parasequences (Fig. 4). The total number of defined IPUs across the study interval decreases northward (down depositional dip) (Fig. 4A). From the total IPUs recognized across the study area, the maximum value was identified in the southernmost region (35 IPUs, section Puesto Leiva), whereas the minimum was identified in the northernmost region (5 IPUs, section El Abra) (Fig. 4A).

Most of the 10 parasequences include up to 3 or 4 IPU (Fig. 4B), but parasequence PS400 exceeds this number with a maximum of 13 IPUs (Fig. 4B). The maximum value observed in PS400 results from the higher resolution of the original study (Fig. 2C). IPUs in PS400 represent up to 60% of the total number of IPUs defined in the section Puesto Riquelme (Fig. 4B). The number of IPUs is uncommonly uniform across the 25-km study area, and it tends to decrease gradually within a single PS from south to north (e.g., PS260, PS300, PS380 in Fig. 4B). The PS400 does not follow this trend because its number of IPUs attains the maximum value in the central sector of the study area (Fig. 4B). In the northern part of the study area (e.g., El Abra section), 8 out of 10 parasequences (80%) cannot be subdivided into smaller scale stratigraphic units (Fig. 4B).

Thickness of IPUs

Although the thickness of individual parasequences varies laterally (Fig. 2), collectively they commonly range from 10 to 50 m, with a mean of 26 m (Schwarz et al. 2018). Stratigraphically, however, the lower parasequences of the studied interval (PS260–PS290) record thicknesses oscillating between 20 and 50 m, whereas the upper ones (PS360, PS380, PS400) range from 5 to 30 m, thus indicating an overall upward thinning of parasequences (Fig. 2).

IPU thicknesses were systematically measured across the studied transect and related to their hosting parasequence. Measured thicknesses plotted along the depositional dip of the transect ranges between 0.5 and 40 m, where values over 40 m represent parasequences in which IPUs were not recognized (Fig. 5A). There is an apparent gap in the thickness values, which defines a boundary between two fields of relatively "thin" (< 20 m thick) and "thick" (> 20 m thick) units (stippled line in Fig. 5A). Considering this division, 95% of the data plot in the "thin" field, whereas only 5% falls in the "thick" field (14 from the total of 274 thickness measurements accumulated from all sections). This empirical boundary is slightly lower towards the offshore and basinal settings. If the same analysis is applied but only considers the sandstone-dominated parasequences, thicknesses of the IPUS range from 0.5 to 25 m and three groups can be established according to the approximate distribution of values: 1) less than 7.5 m thick, 2) between 7.5 m and 15 m thick, 3) more than 15 m thick (Fig. 5B).

Although strong trends are not observed, there is an increase in the thickness values towards the northern localities (distal settings), as identification of IPUs becomes more problematic (Fig. 5A). IPU thicknesses mostly range from 0.5 to 10 m in the southern part of the study area (proximal settings), whereas values oscillate between 2 to 20 m in the northern area (distal settings). Besides, the thickening trend is not necessarily constant for IPUs of the same parasequence. For example, the two upper IPUs of parasequence PS360 thicken northward (IPU360.2 and IPU360.3; Fig. 5C), in consonance with a thinning of the basal IPU (IPU360.1). The northward thickness increase was in some cases caused by the coalescence of two IPUs. In the distal settings (i.e., in the northern part of the study area), where the investigated deposits become mudstone-dominated and more homogeneous, the bounding surfaces (if present and recognized), become more cryptic, and consequently parasequences cannot be subdivided into smaller-scale units (Fig. 3B). The IPU thicknesses can also be analyzed in terms of vertical distribution. If thicknesses of IPUs contained in the same parasequence are evaluated, higher values tend to correspond to the lowermost units (Figs. 5D) whereas the upper ones tend to be thinner.
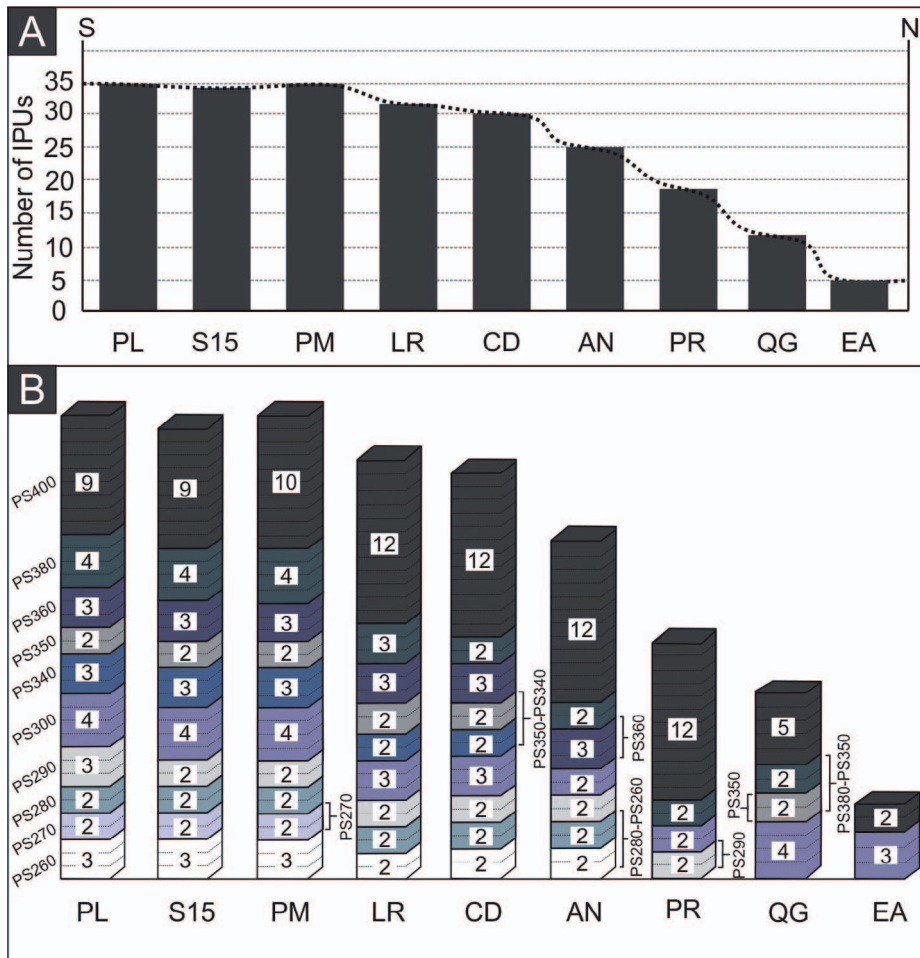
Fig. 4.—**A)** Bar chart showing the cumulative number of intra-parasequence stratigraphic units (IPUs) in the ten parasequences. The number of intra-parasequence units (IPUs) clearly decreases northward (inferred distal part of the basin). **B)** Bar chart specifically indicating the number of IPUs within each parasequence. The brackets indicate groups of IPUs or parasequences that transition laterally to a single unit (with no internal subdivision defined).

Facies Proportion in the Regressive Interval of Each IPU

All the individual IPUs show regressive trends with shallower facies associations towards the top, eventually interrupted by transgressive surfaces (Figs. 2, 3A, B). However, the ideal and complete regressive succession comprising basin (BA), offshore (OF), offshore-transition (OT), lower-shoreface (LS), and upper-shoreface deposits (US) (Table 1) is rarely preserved at intra-parasequence scale. Thus, to further understand the interrelationships between different quantified criteria (e.g., with IPU thicknesses), we first discriminate three main categories of IPU by their thickness proportion to total parasequence thickness, and then we calculate the facies association contribution to a given IPU within the study area (Fig. 6).

Category 1 is defined as IPUs representing less than 15% of total parasequence thickness, and such IPUs are dominantly present where the number of IPUs is four or more (Fig. 6). Thus, this category is mainly recognized in the proximal sector of parasequence PS400 (Fig. 6, PL to AN sections). This category shows the highest proportion of LS+US deposits, representing between 60% to 100% of the entire IPU thickness (81% average). In this category, four of the total 40 IPUs are entirely composed of LS deposits and four of US deposits.

Category 2 was defined for IUPs representing between 15 to 50% of the total parasequence thickness, and they are commonly present where the number of IPUs is three or four (Fig. 6). The LS+US interval is also dominant (40–100% of the entire IPU thickness; 60% average), but OT+OF deposits (41% average of IPU thickness) increase in thickness compared to Category 1 (27% average of IPU thickness; Fig. 6). In a few

cases in this category (9 out of 45), IPUs are composed entirely of offshore deposits.

Category 3 was defined for IPUs representing 50–90% of total parasequences thickness, and thus they tend to be dominant where the number of IPUs is two or three (Fig. 6). Apart from a few rare cases, Category 3 is largely dominated by facies associations representing the distal segment of the marine depositional profile. IPUs of this category are thus mostly composed of OT+OF+BA deposits that most commonly represent 50 to 100% of the entire regressive thickness (88% average; Fig. 6). In 3 out of 34 total cases does the combination of LS+US deposits exceed 50% of regressive thickness (Fig. 6).

Category 4 was defined for parasequences where no internal IPUs can be defined, and thus the single regressive package corresponds to the 100% of the parasequence thickness (e.g., PS270, PS350, PS360 at certain measured sections; see Fig. 6). This category is composed almost entirely of OF+BA deposits, except PS350 in AN, where OT deposits represent 10% of regressive thickness (Fig. 6).

Degree of Deepening (DD) across the IPU Bounding Surface

Transgressive surfaces or a vertical facies transition that indicates deepening is at the core of any sequence-stratigraphic analysis (Van Wagoner et al. 1988, 1990; Cattaneo and Steel 2003; Hampson et al. 2008, 2011; Amorosi et al. 2017; Zecchin et al. 2019). To avoid a subjective approach, emphasis must be placed on semiquantitative assessing the deepening in terms of paleo–water depth. In this paper, the degree of deepening (DD) across a given bounding surface is calculated by the
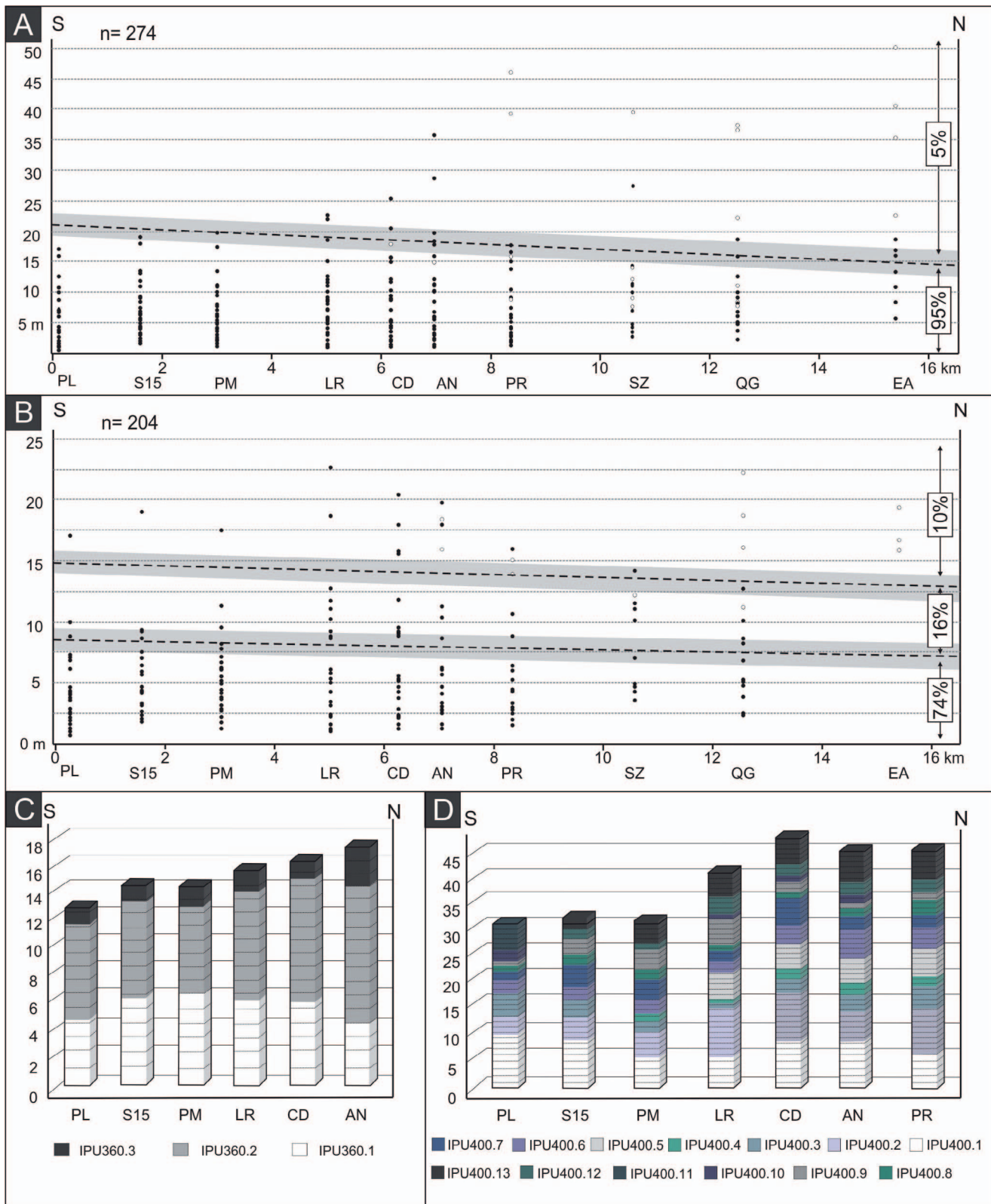
Fig. 5.—A) Thicknesses vs. distance from south (section PL, 0 km) to North (section EA, 18 km) of intra-parasequence units (IPUs), ranging from 0 to 50 m. Black dots: IPUs; White dots: parasequences (no IPUs defined). The dashed line marks the boundary between relative "thin" and "thick" units. Inclination of the line is related to a theoretical seaward decrease in sedimentation rates. B) When thickness analysis is restricted to shoreface-dominated parasequences (more than 40% of the total thickness), values range from 0 to 25 m and it is possible to distinguish three different fields. C) Thicknesses vs. distance from south (section PL) to north (section AN) of IPUs in parasequence PS360. Note that the increased thickness of IPU360.2 compensates for a decrease for the IPU360.1. D) Thicknesses vs. distance from south (section PL) to north (section PR) of IPUs in parasequence PS400, which contains 13 IPUs. The lowermost IPU is commonly thickest.
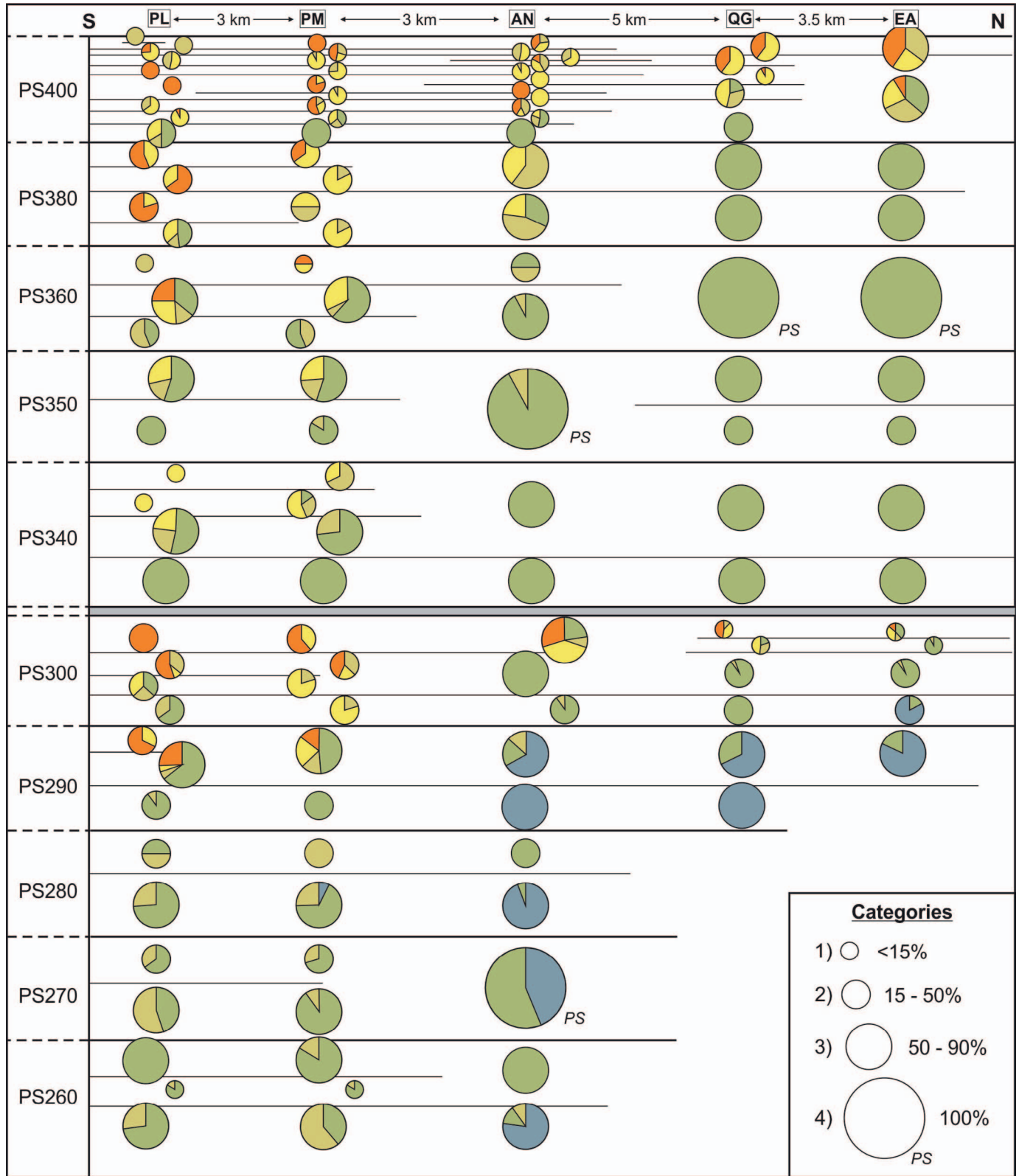
FIG. 6.—Plot documenting the proportion of facies in the regressive intervals of each intra-parasequence unit (IPU). Four sizes of pie charts were defined according to their represented percentage of the parasequence thickness (from small to large pie charts: < 15%, 15–50%, 50–90%, and 100%). Facies associations have the same colors as in Figure 2.

number of facies belts that have been dislocated (Figs. 3A, 7). In this way, this parameter was measured in 198 cases and includes not only the upper boundaries of IPUs within parasequences, but also the upper boundary of the uppermost IPU in each parasequence, which is equivalent to the parasequence-bounding transgressive surface (Fig. 7).

From the total 198 measured vertical facies changes, an OF-OF contact representing a DD0 was the most common and repeated 46 times (23%), an OT-OF contact representing a DD1 was recorded in 34 cases (17%), and LS-OT contact representing a DD2 was observed in 28 examples (14%) (Fig. 7A). The remaining 90 contacts (37%) are represented, in decreasing order, by LS-LS (15), US-LS (14), OF-BA (13), US-OT (12), US-OF (12), LS-OF (10), BA-BA (5), OT-OT (4), US-US (3), and OT-BA contacts (2). As the DD of a given bounding surface was observed to change laterally in most cases (Fig. 7B), the facies dislocation across each surface was also captured by considering the extent of the surface (Fig. 7C).

As expected, the transgressive surfaces interpreted as parasequence boundaries (Table 2) can be easily differentiated using this semiquantitative analysis of the degree of deepening. Such surfaces show a vertical deepening of at least two facies belts in some segments of the study area (DD2), typically towards proximal settings (Fig. 7B). DD2 or DD3 is observed across 20% or more of the lateral extent of parasequence boundaries. In contrast, transgressive surfaces bounding IPUs within parasequences typically show a degree of deepening that is less than two, with the vast majority corresponding to DD1 (10–100%) or DD0 (30–100%) (Fig. 7B). IPU bounding surfaces in parasequence PS400 show the highest concentration of DD2 values (excluding parasequence boundaries), being recorded in seven of the 12 transgressive surfaces (Fig. 7B, C). This parasequence also contains the highest number of IPUs in which Category 1 of regressive deposits is dominant (Figs. 4B, 6).

Previous studies focusing on intra-parasequence (bedset) boundaries remarked that their recognition is spatially limited (Hampson 2000; Hampson and Storms 2003; Storms and Hampson 2005; Sømme et al. 2008; Forzoni et al. 2015), because the DD is commonly 0 in the proximal and distal settings (upper-shoreface and offshore deposits, respectively). In that sense, the identifiability of a bounding surface, as evidenced by the proportion of DD values along their lateral extent, is a useful criterion. IPU bounding surfaces can be empirically separated into two different groups: those where a DD0 is recorded in less than 30% of the bounding surface extent, and those cases where DD0 is recorded in more than 30% of the bounding surface extent (Fig. 7C).

Lateral Extent of IPU Bounding Surfaces

The possibility of pinpointing vertical facies change across a transgressive surface is intimately associated with the degree of deepening (DD) across it and the window in the shoreface–shelf system that we are looking at. The lateral extent of a transgressive surface, in other words the ability to recognize it in the succession, would therefore be higher as DD increases. Its recognition would also be favored by the position in the depositional system, with intermediate segments having the best chances to show more evident vertical facies changes.

As 42 IPUs were originally discriminated in this analysis (Fig. 2), the lateral extent was calculated for 42 upper bounding surfaces of IPUs (Fig. 8). In order to better compare the lateral extent of IPU bounding surfaces, this parameter was represented in each case as a proportion of the lateral extent of the underlying parasequence boundary (Fig. 8). Furthermore, surfaces in sandstone-dominated and mudstone-dominated parasequences were differentiated.

According to their relative lateral extent (compared to the lateral extent of the underlying parasequence boundary), three main types of surfaces are established: a) "short surfaces" (< 0.7 for sandstone-dominated parasequences and < 0.5 for mudstone-dominated parasequences); b) "intermediate surfaces" (> 0.7 and < 1 for sandstone-dominated

parasequences and, > 0.5 and < 1 for mudstone-dominated parasequences); and c) "extensive surfaces" (equal to 1). These results indicate that most IPU bounding surfaces correspond to the "short-surfaces" type (50%), whereas some of them fall in the "intermediate-surfaces" type (19%) (Fig. 8A). Apart from surfaces TS300.1 and TS400.10, the "extensive-surfaces" type corresponds invariably to parasequence boundaries (Fig. 8). If only sandstone-dominated parasequences are considered, 64% of the 25 measured surfaces correspond to "short surfaces," whereas "intermediate surfaces" represent 16%. For mudstone-dominated parasequences, 29% of the 17 total surfaces were assigned as "short surfaces" and the 23% to "intermediate surfaces."

Type and Lateral Extent of Thin Transgressive Deposits

The shell beds facies associations (SSB and OSB in Table 1) are invariably associated with surfaces bounding genetic units in the investigated succession, and they typically represent thin transgressive deposits formed in shoreface to offshore settings (Figs. 2, 3). Thus, in order to explore if the presence, type, and/or vertical and lateral facies transitions of these transgressive deposits can be used as a predictive tool for the nature of the IPU bounding surfaces, we quantified these parameters across the study area (Fig. 9).

The resulting analysis (from a total of 42 bounding surfaces) allowed discrimination between different stratigraphic scenarios. In 43% of cases, transgressive surfaces are directly overlain by SBB deposits (66% of them from the IPUs of the PS400), and only in 9% of cases (four from 42) is there a lateral transition into the OSB facies association. These cases may correspond to IPU boundaries (Fig. 9), and typically correlate with units that show clear shoreface-to-offshore facies lateral transitions. In 20% of the total cases, corresponding either to PS or IPU boundaries, the OSB deposits are demarcating the bounding surfaces, and this correlates well with units where OT, OF, and BA deposits are dominant. In the 9% of the cases (four from 42) there is a clear retrogradational hemicycle with SSB deposits at the base, grading both vertically and laterally to the OSB facies association. This type of more complex transgressive deposit is more commonly observed at parasequence boundaries. In the remaining cases (28%) the bounding surface is not demarcated by shell-bed deposits in the study area.

HIERARCHY OF HIGH-RESOLUTION STRATIGRAPHY AND EVALUATION OF CRITERIA

Proposed Hierarchy for the Pilmatué Member

The quantitative analysis developed in this contribution allows recognition of a hierarchy of intra-parasequence stratigraphic units in the Pilmatué Member. The northward decrease in the number of IPUs observed in the studied interval, until no subdivisions are identified in a single parasequence, fits with general trends described for distal settings in other ancient examples (Sømme et al. 2008; Hampson et a. 2011; Zecchin et al. 2017). However, the gradual trend presented here for this parameter (Fig. 4A) challenges the existence of a unique order of hierarchy (i.e., bedset) at intra-parasequence scale.

The presence of more than one scale of IPU becomes more evident when several parameters are combined and analyzed in a several-km-long cross section, as presented here (Fig. 3). Apart from parasequences, which have already been identified, three different scales of IPU are defined in the study interval, all having coarsening- and shallowing-upward vertical trends: bedset complexes, bedsets, and sub-bedsets. Most of the intra-parasequence stratigraphic units previously interpreted as bedsets (Isla et al. 2018; Schwarz et al. 2018), fall within the intermediate hierarchy (Table 3), whereas some are re-assigned to bedset complexes, and others are identified as sub-bedsets (Fig. 10A–C). Intra-parasequence bounding surfaces of successive hierarchies show a concave-upward geometry
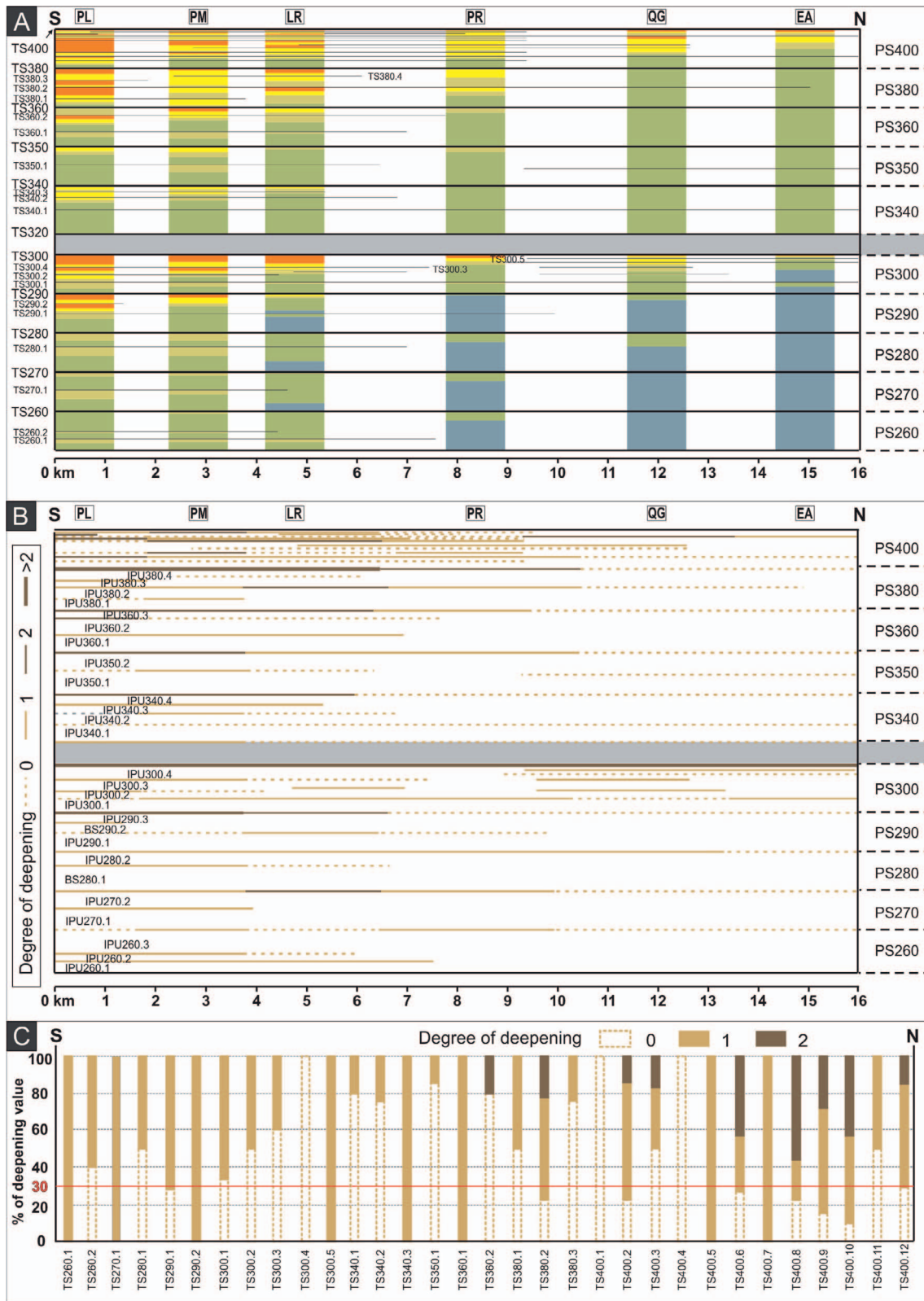
Fig. 7.—**A)** Degree of deepening (DD) across transgressive surfaces bounding parasequences and intra-parasequence units (IPUs) (e.g., TS350 represents a parasequence boundary and TS350.1 represents a IPU boundary). **B)** Plot showing the degree of deepening across the transgressive surfaces, expressed in terms the number of facies associations that have been dislocated across the surface. **C)** Proportion of values of the degree of deepening determined for each IPU bounding surface (parasequence boundaries were excluded from the analysis).
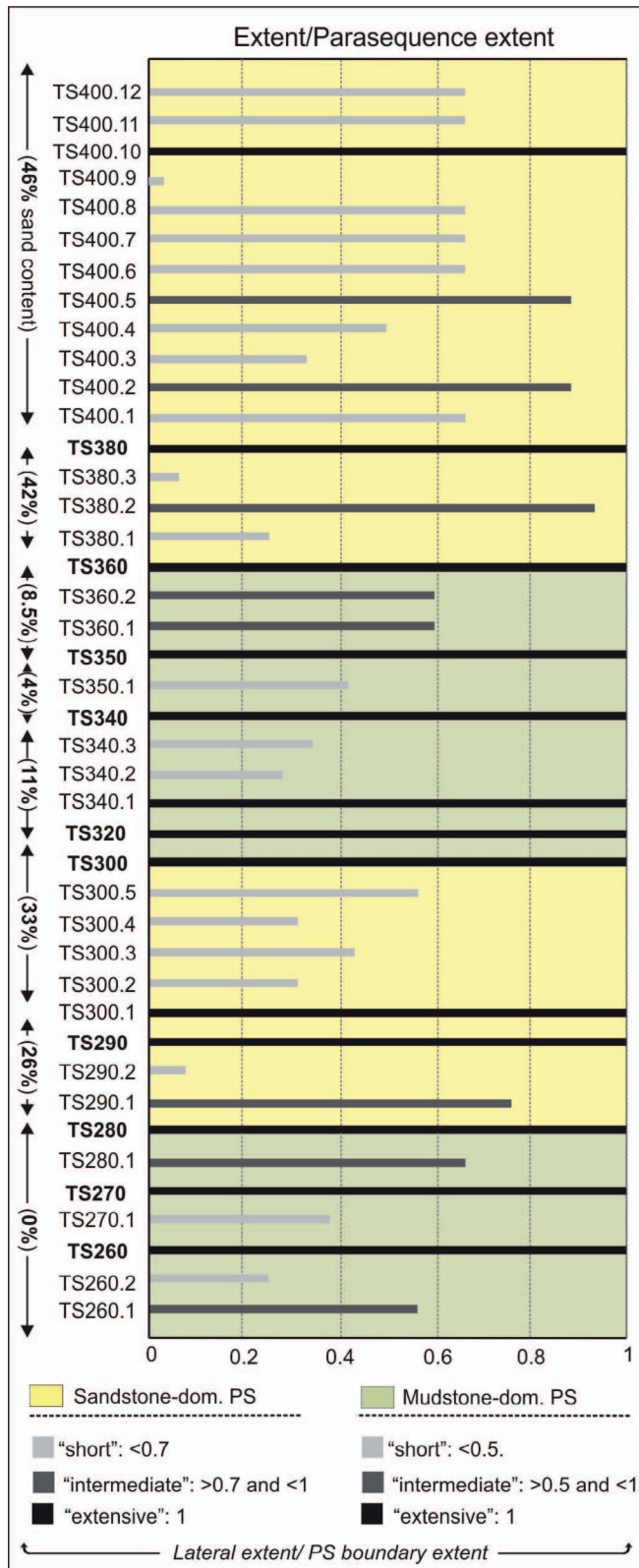
FIG. 8.—Lateral extent of all the identified bounding surfaces measured along the studied 16-km north–south-oriented transect (see Fig. 1 for location and Fig. 2 for detailed facies distribution). Surfaces can be divided into three groups: "short" (pale gray lines), "intermediate" (medium gray lines), and "extensive" surfaces (dark gray lines). Surfaces were also differentiated between those in sandstone-dominated parasequences (i.e., sections dominated by lower- to upper-shoreface deposits) and in mudstone-dominated parasequences (i.e., sections dominated by offshore-transition to basinal deposits).

resembling to a shoreface–shelf profile, where steepest sections typically occur in proximal settings (shoreface deposits). However, these surfaces (clinoforms) are roughly parallel to parasequence boundaries (Fig. 10), which differ from the typical wedge-shaped geometrical configuration for shoreface–shelf systems (Storms and Hampson 2005; Hampson et al. 2008; Patruno et al. 2015). This is also supported by relatively low thickness variations in parasequences between proximal and distal settings (Fig. 10). Contrary to the typical wedge-shaped architecture where successions commonly thin towards distal settings and hence, chronostratigraphic surfaces tend to be vertically condensed, the reconstructed architecture for the upper half of the Pilmatué Member suggests that thickness, and thus time, is approximately evenly distributed from proximal to distal segments of the depositional profile. This unusual longitudinal pattern has been attributed to a combination of a carbonate contribution in basinal settings (Schwarz et al. 2018; Remirez et al. 2020).

Parasequences (PS).—Quantitative attributes collected for the parasequences of the Pilmatué Member reinforce their previous interpretation as the fundamental high-resolution stratigraphic units (Schwarz et al. 2018). These 10–50-m-thick (Fig. 11) successions are bounded by transgressive surfaces with associated shell bed deposits. Parasequences typically record the complete offshore to upper shoreface progradational succession at least in one section of the study area (Fig. 6), but in the northern sector they might be composed entirely of offshore and basinal deposits (Fig. 11). The regular presence of shell bed deposits (40% of SSB+OSB and 60% of OSB), which are interpreted to be transgressive, indicates that the identified parasequences fit better with the definition of high-frequency sequences (Zecchin and Catuneanu 2013; Schwarz et al. 2016b; Zecchin et al. 2017). The maximum degree of deepening is typically three, decreasing towards distal areas (Fig. 11). Parasequence boundaries represent the most extensive surfaces identified here, being traceable for up to 20 km, i.e., over the entire study area (Figs. 2, 8), but may lose expression in terms of facies change towards the northern part of the study area (e.g., in sections El Abra and San Eduardo).

Bedset Complexes (BCs).—These 10–40-m-thick stratigraphic units represent the highest hierarchy of intra-parasequence stratigraphic units (Fig. 11). The vertical stacking of two or three bedset complexes conforms to an individual parasequence (Fig. 11A). The bedset complexes become more evident towards intermediate to distal depositional settings where offshore-transition and offshore deposits commonly dominate (Fig. 11B, C). Detailed, high-resolution lateral analysis allows recognition of bedset complexes in offshore and basinal deposits, as has been suggested for mudstone-dominated parasequences (Bohacs et al. 2014). Bounding surfaces of bedset complexes extend between 5 and 16 km, which fits in the "intermediate surfaces" category (Fig. 8) defined in this study (representing 60–100% of the extent of parasequence boundaries; Fig. 8). The degree of deepening across bounding surfaces of bedset complexes commonly indicates a vertical shift of one facies belt at least along 70% of their extent (with a maximum of three facies belts; Fig. 7C). These transgressive surfaces are commonly associated with shell beds (30% of them contain both SSB and OSB), displaying evidence of wave reworking in proximal settings (i.e., defining wave-ravinement transgressive surfaces), but only stratigraphic condensation towards distal settings (Fig. 11). In some cases, the assignation to bedset complexes still needs to be confirmed (e.g., BC350.1 and BC350.2), because they do not exhibit internal bedsets in the study area (although such bedsets may be recorded beyond the southernmost section; Fig. 10).

Bedsets (Bs).—Bedsets are 2–20-m-thick successions (Fig. 11), and two or three bedsets are vertical stacked to build a bedset complex (Fig. 12A, B). In general, bedsets are composed mainly of lower-shoreface and
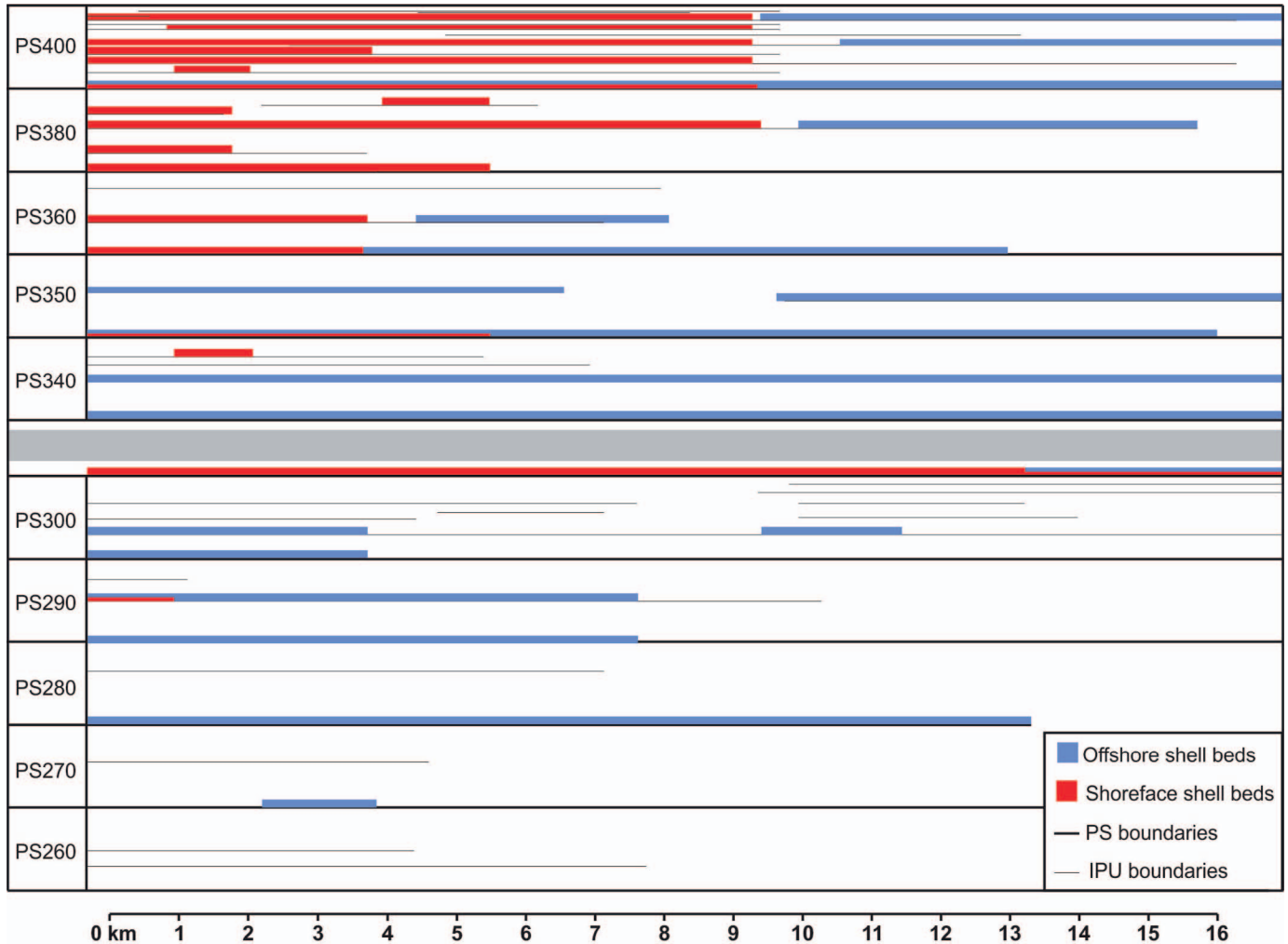
Fig. 9.—Distribution of shell-bed deposits associated with bounding surfaces.

offshore transition deposits (50% to 100% of the preserved record) with subordinate upper-shoreface facies. Exceptionally, bedsets may be composed entirely of offshore deposits (Fig. 6), commonly in the lowermost part of a parasequence. Internally, bedsets may record the vertical stacking of up to four facies associations (e.g., OF-OT-LS-US).

The boundaries of bedsets were mapped up to 10 km laterally (Fig. 2), corresponding to "short" or "intermediate surfaces" (representing 5–50% of the extent of parasequence boundaries; Fig. 8). Besides, bedsets may be associated with the presence of shell beds (54%) or not (46%). Where present, shell beds correspond to SSB (39%) or SSB laterally transitioning to OSB deposits (15%), which also depends on the underlying facies associations. The degree of deepening across bedset bounding surfaces is commonly 0–1 and this value can be consistent along most of a surface's

extent (70%, Fig. 7B). In proximal settings, where upper-shoreface deposits are common, the degree of deepening varies from 0 to 2 (Fig. 7A). Where bedset boundaries lack vertical facies changes in such proximal settings (Fig. 7A), their recognition depends on the presence of SSB deposits. From the total of 42 defined IPUs in the Pilmatué Member, 24 correspond to bedsets (Table 3).

Sub-Bedsets (SBs).—The stratigraphic units representing the highest order of IPUs is here named sub-bedsets because they are defined within bedsets (Fig. 11). The sub-bedsets are mostly confined to parasequence PS400 (Figs. 2C, 12B), in which the most detailed stratigraphic studies have previously been carried out (Isla et al. 2018, 2020a, 2020b), but a few IPUs with similar attributes were identified in other parasequences (e.g.,

TABLE 3.—*New intra-parasequence stratigraphic framework of the upper half of the Pilmatué Member. *The reassignment of IPUs as BCs still require the identification of their constituent Bs.*

| IPUs reassigned to sub-bedsets	IPUs kept as bedsets	IPUs reassigned to bedset complexes*
IPU400.4, IPU400.5, IPU400.6, IPU400.7, IPU400.8, IPU400.9, IPU400.10, IPU400.11, IPU400.12	IPU260.2, IPU260.3, IPU270.1, IPU270.2, IPU290.2, IPU290.3, IPU300.2, IPU300.3, IPU300.4, IPU300.5, IPU300.6, IPU340.2, IPU340.3, IPU340.4, IPU360.1, IPU360.2, IPU380.1, IPU380.3, IPU380.3, IPU380.4, IPU400.1, IPU400.2, IPU400.3, IPU400.13	IPU260.1, IPU280.1, IPU280.2, IPU290.1, IPU300.1, IPU340.1, IPU350.1, IPU350.2, IPU360.3
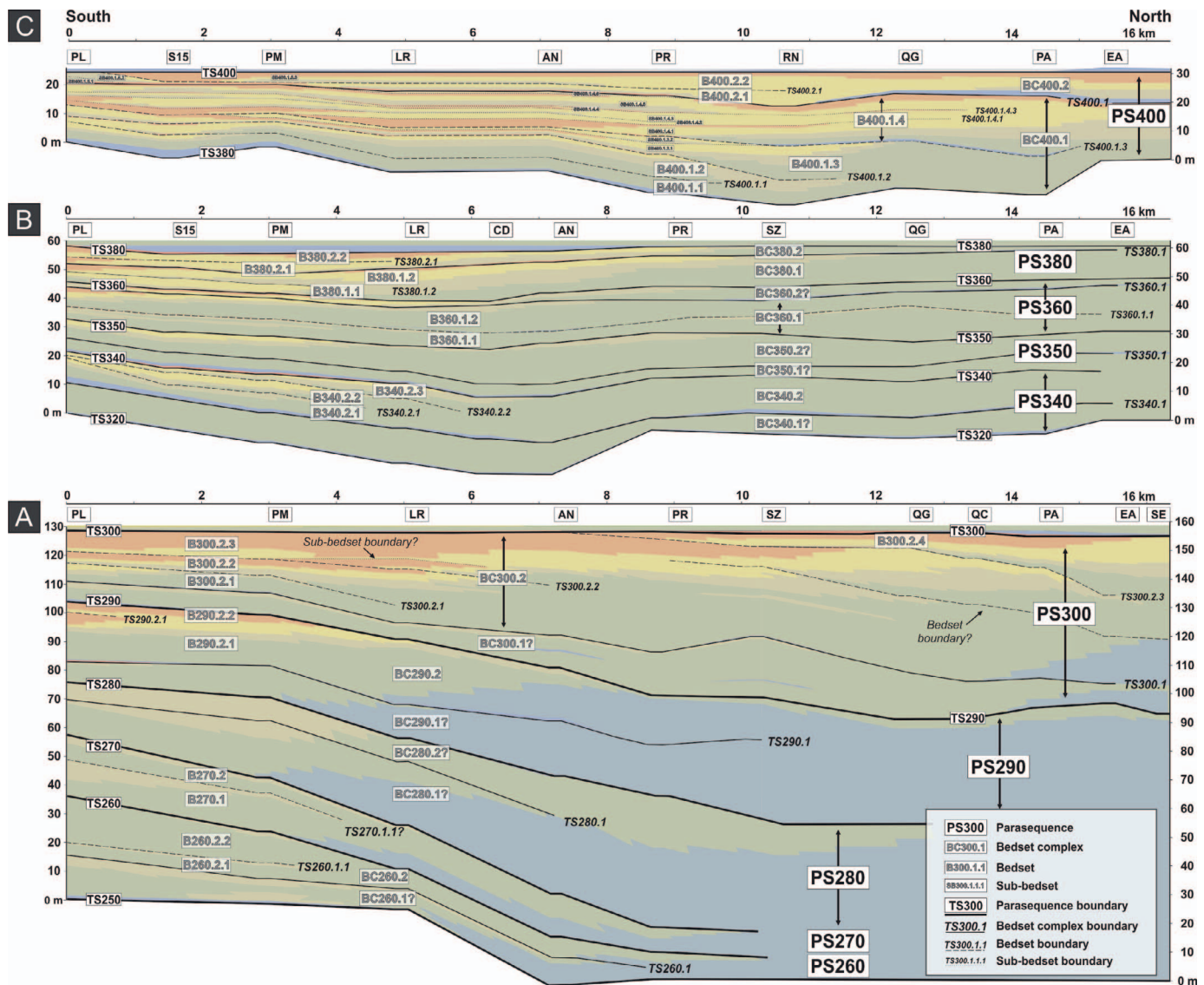
FIG. 10.—Sequence-stratigraphic architecture of the upper half of the Pilmatué Member, illustrating the hierarchy of intra-parasequence genetic units (IPUs) defined in this paper. **A)** PS260 to PS300, **B)** PS340 to PS380, **C)** PS400. Bedset complexes (BCs) with a query still have to be confirmed, since they do not contain bedsets in the study area. Flattening datums: A) TS300, B) TS380, C) TS400. Facies associations have the same colors as in Figure 2.

PS300). Sub-bedset thicknesses vary between 0.5 to 5 m (Fig. 5B). Two or three sub-bedsets commonly stack to form bedsets and their individual identification clearly decreases as facies become more distal (e.g., the 11 sub-bedsets defined in the proximal settings of parasequence PS400 merge seaward into four bedsets; Fig. 6).

Sub-bedsets are typically composed of lower- and upper-shoreface deposits, with subordinate proportions of offshore-transition facies (Fig. 6). The lateral extent of their bounding surfaces is relatively low (0.5–2 km), equivalent to the "short surfaces" defined in Figure 8, but occasionally can reach 10 km (e.g., TS400.8; Fig. 8). The degree of deepening across the bounding surfaces is 0–1 (for 80–100% of their extent), but DD values of two were also recorded in proximal depositional settings (Fig. 7B, C). Sub-bedset boundaries are almost invariably associated with wave-ravinement surfaces and thin SSB deposits (80%) in sandstone-dominated deposits (US and/or LS facies associations). These shell beds rapidly pinch out towards more distal deposits, where sub-bedset's bounding surfaces become hard to identify because the degree of deepening across them is

commonly zero (Fig. 11). OSB deposits were not found along sub-bedset boundaries. Apart from the sub-bedsets recognized in PS400, the rare apparent occurrence of sub-bedsets suggests that their recognition is directly related to the scale and detail of study and the presence of proximal (shoreface) deposits.

The Toolbox for Discriminating IPUs: A Set of Criteria

The quantitative parameters presented in this study helped in recognizing a three-fold hierarchic scheme of intra-parasequence units (bedset complexes, bedsets and sub-bedsets), but importantly, not all the criteria are equally effective for discriminating between these different categories (Fig. 13A). In addition, the efficacy of each criterion depends directly on the dataset and resolution, as well as the specific characteristics of the basin (e.g., the applicability of shell beds is inherent to depositional systems in which there is mixing between terrigenous material and skeletal fragments and/or in which carbonate is preserved during diagenesis). Collectively, all these results suggests that if a given parasequence can be
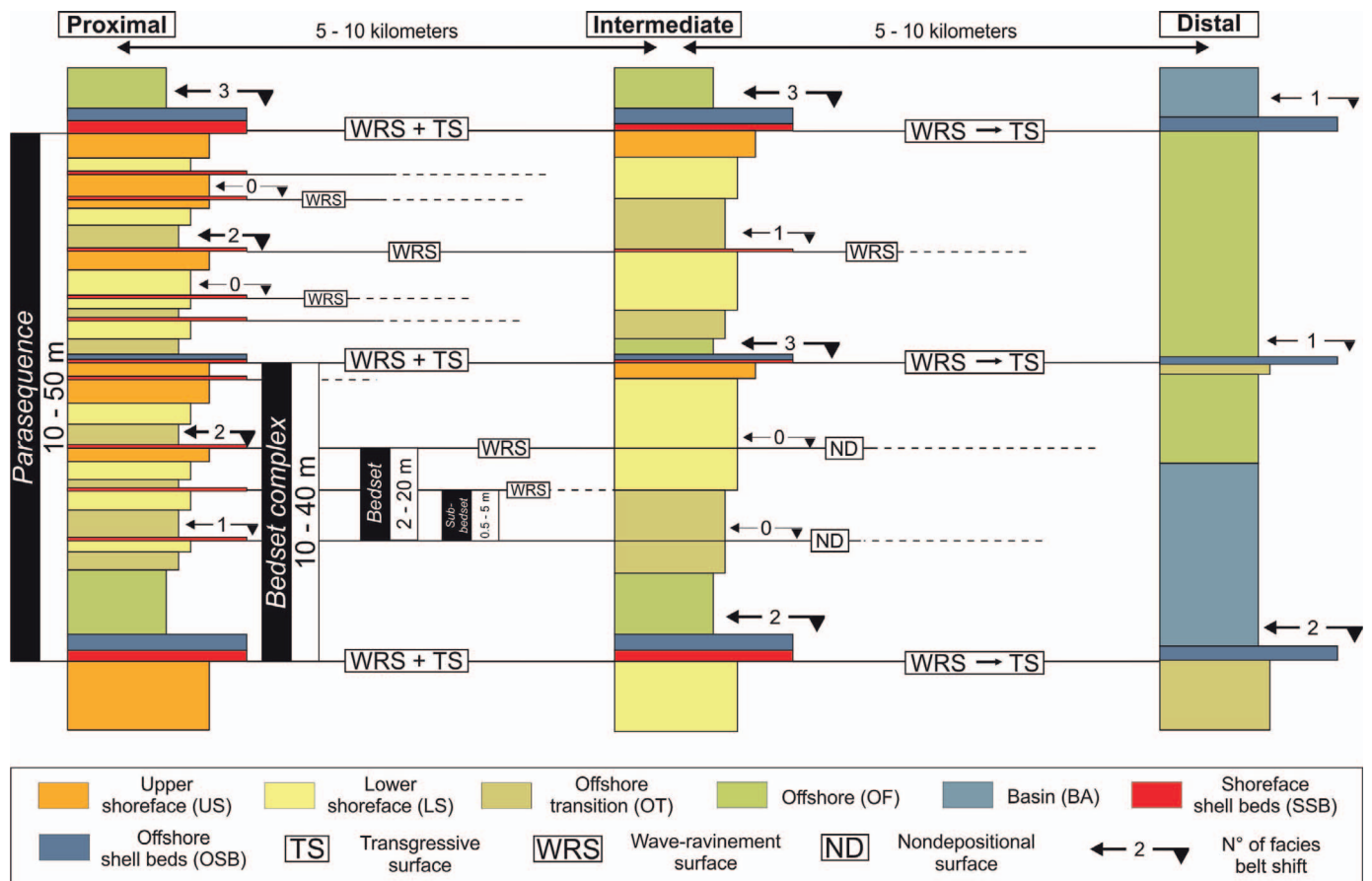
FIG. 11.—Conceptual model summarizing the intra-parasequence hierarchy recognized for the investigated parasequences of the Pilmatué Member. Sub-bedsets are the highest order of the identified intra-parasequence genetic units (IPUs) and typically form regressive successions bounded by erosional or nondepositional surfaces that may extend laterally from 0.5 to 2 km. Sub-bedsets were exclusively recognized in parasequence PS400. The vertical stacking of two or three sub-bedsets form bedsets. These 2–20-m-thick units are bounded by wave-ravinement or transgressive surfaces that may extent for over 5 to 10 km. Bedset complexes are 10–40-m-thick coarsening-upward units extending laterally for 8 to 15 km, forming minor transgressive to regressive cycles. Bedset complexes are commonly associated with shoreface shell beds in proximal settings, which may transition to offshore shell beds farther basinward. Finally, bedset complexes may stack into parasequences, which constitute 10–50-m-thick (composite) coarsening-upward units extending laterally for 10 to 20 km. Parasequences conform to high-frequency transgressive to regressive cycles bounded by transgressive surfaces.

subdivided into smaller units, it might not necessarily indicate that all of them are of the same hierarchical level. Moreover, this approach suggests that the resulting hierarchical scheme of IPUs (i.e., number of units of different scales) is directly related to the available datasets. For example, the recognition of sub-bedsets would be possible if detailed depositional and stratigraphic information is available in dense datasets (e.g., lateral sampling of 500 m or less). In turn, the identification of larger-scale units (bedsets and bedsets complexes) would be possible to identify with less dense datasets (e.g., when lateral sampling is 1–5 km).

According to this study, the thickness attribute represents a first approximation to discriminate between different IPUs. Apart from the previously defined parasequences (10–50 m), the three hierarchic units recognized here show the following thickness ranges: bedset complexes (10–40 m), bedsets (2–20 m), and sub-bedsets (0.5–5 m). Despite an expected overlapping, these data suggest that the thicker the IPU, the higher its position in the hierarchy of the units (Fig. 13B). However, discrimination between these three hierarchically different stratigraphic units becomes clearer when average values are calculated. Average thickness is 12 m for bedset complexes, 5.5 m for bedsets, and 3.6 m for sub-bedsets (Fig. 13B). Considering these results, the thickness attribute, which is easily obtained from 1D or 2D datasets, is a useful

approximation and can be used as a first diagnostic criterion, but it should be complemented with other criteria to build a hierarchy of IPUs.

The combination of IPU thickness with its proportion of facies associations in the regressive interval offers an even better discrimination of IPU categories. Sub-bedsets are not only the thinnest units but also the ones with the highest contribution of sand-rich, lower- and upper-shoreface deposits, where only a minor contribution of offshore-transition facies is recorded (Fig. 13C). Bedsets show a similar contribution of facies, but offshore-transition and offshore deposits are more abundant. For example, a 4-m-thick IPU could be assigned to either a bedset or a sub-bedset. However, if US deposits represent more than 50% of an IPU's thickness and the remaining strata are composed entirely of LS deposits, this IPU would more likely correspond to a sub-bedset as defined in this case study. On the contrary, if the same 4-m-thick IPU is composed of about 50% of US sediments, but in the remaining strata the OT deposits are abundant (e.g., > 20%), the unit could be attributed to a bedset as defined in this case study. Such differences increase for bedset complexes, which can be composed entirely of offshore deposits and, in some cases, basinal facies (Fig. 13C). The bedset complexes may record up to four facies associations in their regressive interval, but this number decreases in distal settings.

Bounding-surface characteristics probably provide the most trustworthy criteria for the definition of IPUs, both in outcrop and subsurface studies.
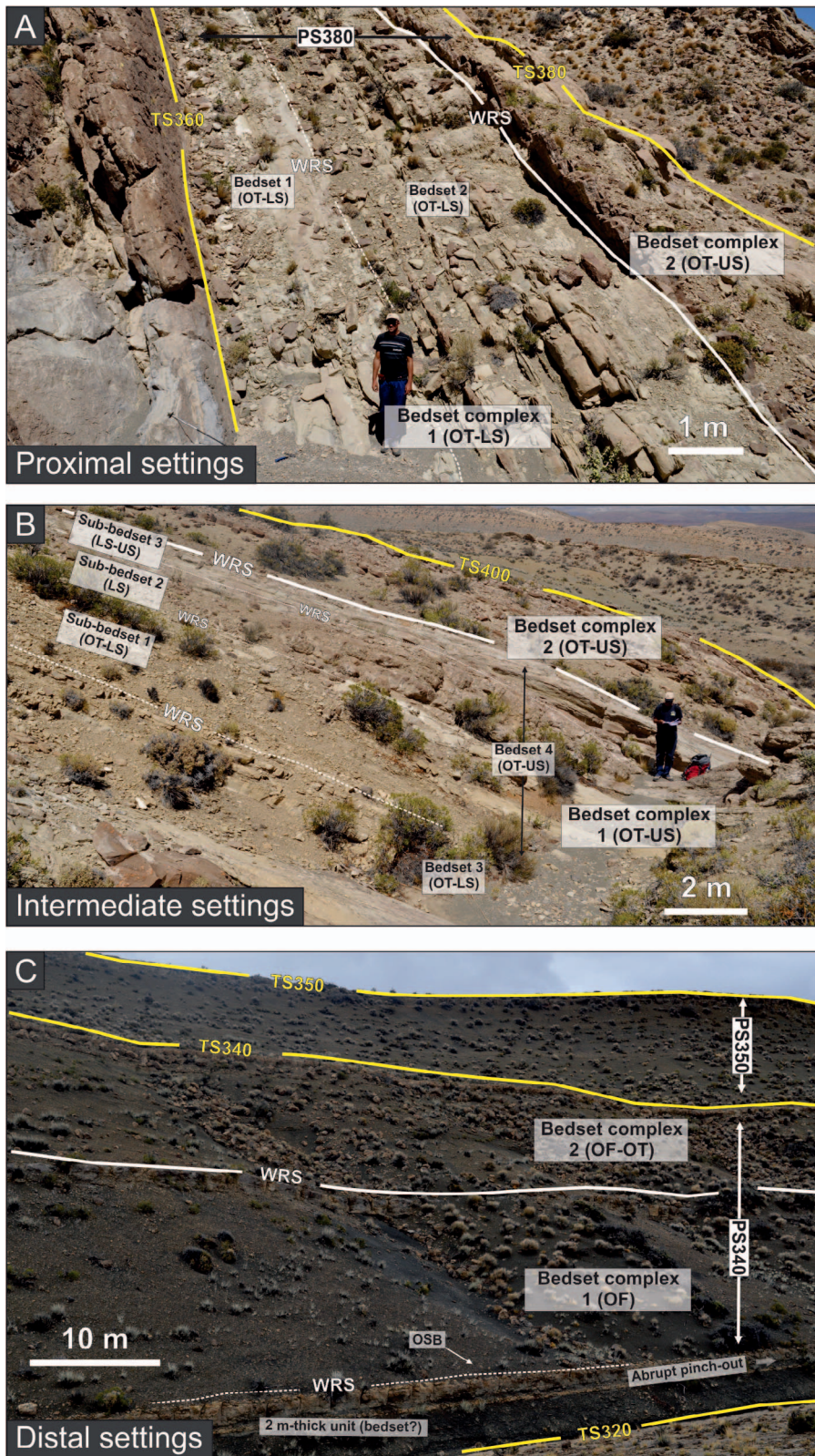
Fig. 12.—Outcrop view showing the recognized intra-parasequence stratigraphic units and their respective bounding surfaces. **A)** Reinterpretation of the parasequence PS380 recording proximal settings (section PM, Figs. 2, 10; modified from Schwarz et al. 2018). **B)** Reinterpretation of the parasequence PS400 recording intermediate settings (section AN, Figs. 2, 10). **C)** Re-interpretation of the parasequence PS340 recording distal settings (section CD, Figs. 2, 10). OF, offshore; OT, offshore transition; LS, lower shoreface; US, upper shoreface; OSB, offshore shell beds.
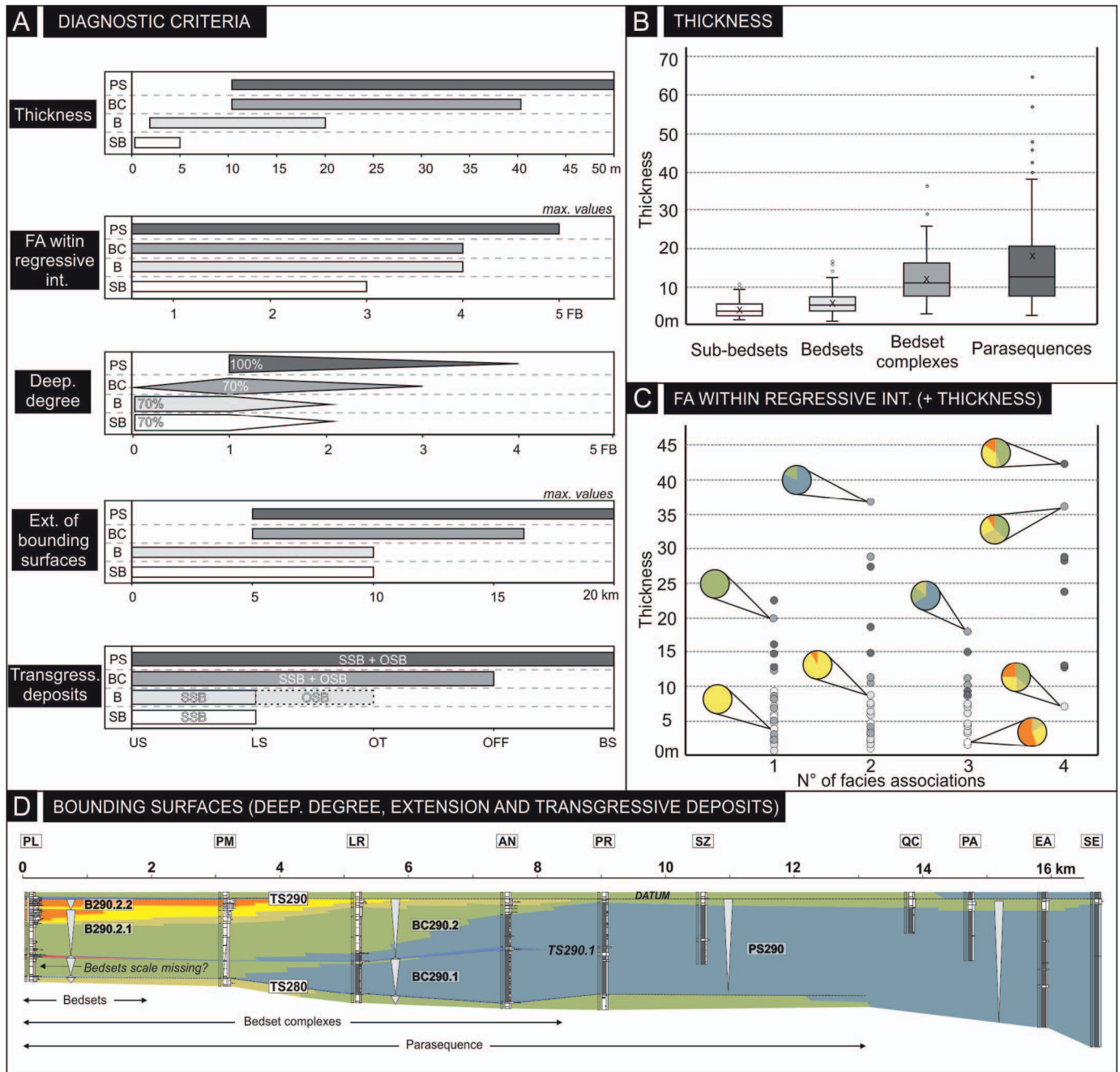
FIG. 13.—**A)** Diagnostic criteria used for defining various scales of intra-parasequence stratigraphic units (IPUs) and distinguishing them from parasequences. **B)** Estimated ranges of thickness for each hierarchy of stratigraphic unit, from sub-bedsets to parasequences. **C)** Relationship between thickness and proportion of facies associations in the regressive part of a stratigraphic unit. Circle colors refer to the units of Part A. **D)** Cross section of parasequence PS290 demonstrating the lateral nesting of successively high-frequency IPUs, giving rise to a composite architecture. SB, sub-bedsets; B, bedsets; BC, bedset complexes; PS, parasequence.

The associated vertical shift of facies across a bounding surface is a key parameter for distinguishing between types of bounding surfaces, and hence determining the hierarchy of the bounded stratigraphic units, but significant uncertainty remains in their expression across the depositional profile. Our data suggest that the combination of degree of deepening, lateral extent of bounding surfaces, and the characteristics of associated shell bed deposits represent an excellent set of criteria for defining parasequences in the Pilmatué Member and discriminating some of the different scales of IPUs within them (parasequences, bedset complexes,

bedsets). For example, if an IPU is bounded by a transgressive surface mappable for 7 km it could be assigned to any hierarchical unit defined in this contribution (Fig. 13A). However, the presence of OSB deposits overlying the surface would exclude the possibility of the underlying unit being a sub-bedset and significantly reduces its chances of being a bedset (only 15% of the defined bedset boundaries exhibit OSB deposits). Moreover, if the 7 km extent of this example surface is large relative to the extent of the parasequence that contains it (70% for sandstone dominated or 50% for mudstone dominated), and the degree of deepening across the

surface is dominantly represented by a shift of one facies belt (i.e., DD1), the underlying unit would likely be a bedset complex (Fig. 13A). However, the bounding surfaces of bedsets and sub-bedsets share similar values of extent, degree of deepening, and shell-bed characteristics: bounding surfaces are typically < 10 km in extent, are marked by low degree-of-deepening values across them (DD1 to DD0), and are commonly overlain by SSB deposits (Fig. 13A).

The lateral distribution of facies and mapping of transgressive surfaces show a clear nesting of successive orders of stratigraphic units. According to the proposed high-resolution stratigraphy for the Pilmatué Member (Fig. 10), a typical parasequence (e.g., PS290) would be composed of two bedset complexes, and in turn the upper bedset complex would contain two bedsets (Fig. 13D). The bounding surface separating both bedset complexes would extend for several kilometers and be associated with SSB deposits in proximal settings, but rapidly grade to OSB deposits in distal settings. In the intermediate area of the cross section, the transgression would be recorded by a small degree of deepening (DD1) from offshore to basin deposits that becomes less marked (DD0) in both updip and downdip directions (Fig. 13D).

In summary, the combined criteria of IPU thickness and facies proportion in the regressive interval of an IPU are required for discriminating IPUs of different hierarchical level when only limited, one-dimensional data are available (e.g., cores, well logs, poorly exposed outcrops). In contrast, the combination of the criteria inherent in bounding surfaces (degree of deepening, extent, and shell-bed characteristics) requires robust two-dimensional information (e.g., outcrop panel, as in this study), which may not be available in many cases. The evaluation of diagnostic criteria for different IPU categories also needs to consider the position across the shoreface–shelf profile that is represented by the strata. Discrimination between bedsets and sub-bedsets is spatially limited to the proximal and intermediate parts of the system, where these small-scale units are easier to identify (Figs. 12A, B). In these proximal settings, bedsets and sub-bedsets can be differentiated by their average thickness and the relative proportion of OT deposits, which are both higher in bedsets (Fig. 13A). Moreover, distinguishing between bedset complexes and bedsets is difficult in proximal settings if interpretations are based only on bounding-surface characteristics. The proportion of facies associations in the regressive interval of an IPU becomes critical in intermediate to distal settings, where bedset complexes are discriminated by being composed chiefly of offshore and offshore-transition facies (Fig. 12B, C). A holistic analysis of the shoreface–shelf profile is even more important to distinguish between bedset complexes and parasequences, which differ in their bounding-surface extents and associated degree of deepening (Fig. 12C). The difficulty in distinguishing between these two types of units is reflected in previous discussions of parasequence definition (Hampson et al. 2008; Amorosi et al. 2017; Zecchin et al. 2017; Colombera and Mountney 2020).

DISCUSSION

Controls on Intra-Parasequence Architecture: Wave Climate or Relative Sea-Level Changes?

High-resolution sequence stratigraphic interpretation, particularly at intra-parasequence scale, requires a balance between evaluating the geological expression of key stratigraphic surfaces, the resolution of data acquisition, and the hierarchy of change associated with the generation of stratigraphic discontinuities. Depending on the scale of defined stratigraphic units, different forcing mechanisms, like relative sea-level oscillations, sediment-supply changes, climate variations, or subsidence, may be invoked. Climatic variations commonly impact over the transport dynamics of coastal environments through changes in the wave climate,

which involve the attributes of waves and currents. Bounding surfaces of successive high-frequency units may result from these changes, potentially leaving a detectable signature depending on bathymetric position in the shoreface–shelf system (Fig. 14).

It is crucial when working with the characterization of intra-parasequence stratigraphic units not to fall into simplistic interpretations. Simplifications may be generated if the resolution data is not enough to identify subtle sedimentologic changes associated with bounding surfaces. Discontinuities typically become more cryptic mostly towards distal settings. For example, our data demonstrate that bedset boundaries tend to become cryptic in the shoreface, where they are commonly represented by a sand-to-sand contact (LS-LS or US-LS). This lack of lithological contrast does not necessarily mean the absence of a bounding surface, which can be evidenced in the shoreface by subtle changes in bioturbation intensity, storm-bed amalgamation (Hampson 2000; Hampson and Storms 2003; Sømme et al. 2008; Forzoni et al. 2015), and/or the presence of shell-bed deposits (Isla et al. 2018). In distal settings, bounding surfaces may be poorly expressed because there is little lithological or facies contrast across them (e.g., subtle transitions from siltstones to mudstones in offshore settings) or absent because they were not generated in distal locations (Fig. 14). The sedimentological evidence of stratigraphic surfaces is intimately related to the nature and scale of their triggering mechanisms.

Previous detailed studies in the Pilmatué Member, focusing on the processes involved during transgression and the shoreline orientation, postulated that sub-bedset boundaries were generated by alongshore imbalances in the sediment budget due to changes in wave climate (Isla et al. 2018). The development of the SSB deposits was interpreted as the result of wave-ravinement processes during transgressions. Hence, the generation of sub-bedset boundaries seems to be controlled by the influence of waves in shoreface to offshore-transition settings (Isla et al. 2018). Though the proposed model for the generation of sub-bedsets focuses on the effectiveness of longshore currents, other types of variations in wave climate could be responsible for their generation. The generation of sub-bedsets is thus more feasibly explained as the result of high-frequency climatic variations (Fig. 14), rather than eustatic and/or tectonic changes.

Bedset boundaries are commonly associated with marked changes in bioturbation intensity, storm-bed amalgamation, and/or differential cementation (Hampson 2000; Hampson and Storms 2003; Charvin et al. 2010; Hampson et al. 2011; Forzoni et al. 2015; Zecchin et al. 2017). Two different types of bedset boundaries have been typically defined for shallow-marine strata: erosional and nondepositional discontinuities (Hampson 2000). Observations on the attributes of both types of boundaries led some authors to postulate that their occurrence depends on vertical movements of fair-weather and storm wave base (Hampson 2000; Hampson and Storms 2003; Storms and Hampson 2005). However, the bedset boundaries in the Pilmatué Member are marked by SSB deposits that grade seaward from wave-ravinement (erosional) to nondepositional (non-erosional) surfaces (Isla et al. 2018). Their lateral extent suggests a widespread influence of the triggering mechanisms during transgressions and hence, high-frequency oscillations in relative sea-level or wave-climate variations (e.g., alterations in wave-angle approach and longshore transport dynamics; Isla et al. 2018) are the most feasible explanations for the generation of bedset boundaries (Fig. 14).

The recognition of bedset-complex bounding surfaces in offshore and basinal settings, favored by the presence of offshore shell beds, suggests that these flooding events affected most of the shoreface–shelf profile. Modeling work focusing on the development of intra-parasequences surfaces demonstrated that relative sea-level changes preferentially affect the proximal settings, whereas variations in wave-base levels produce discontinuities with greater proximal-to-distal extent (Storms and Hampson 2005) as occurs with boundaries of bedset complexes (Fig. 14).
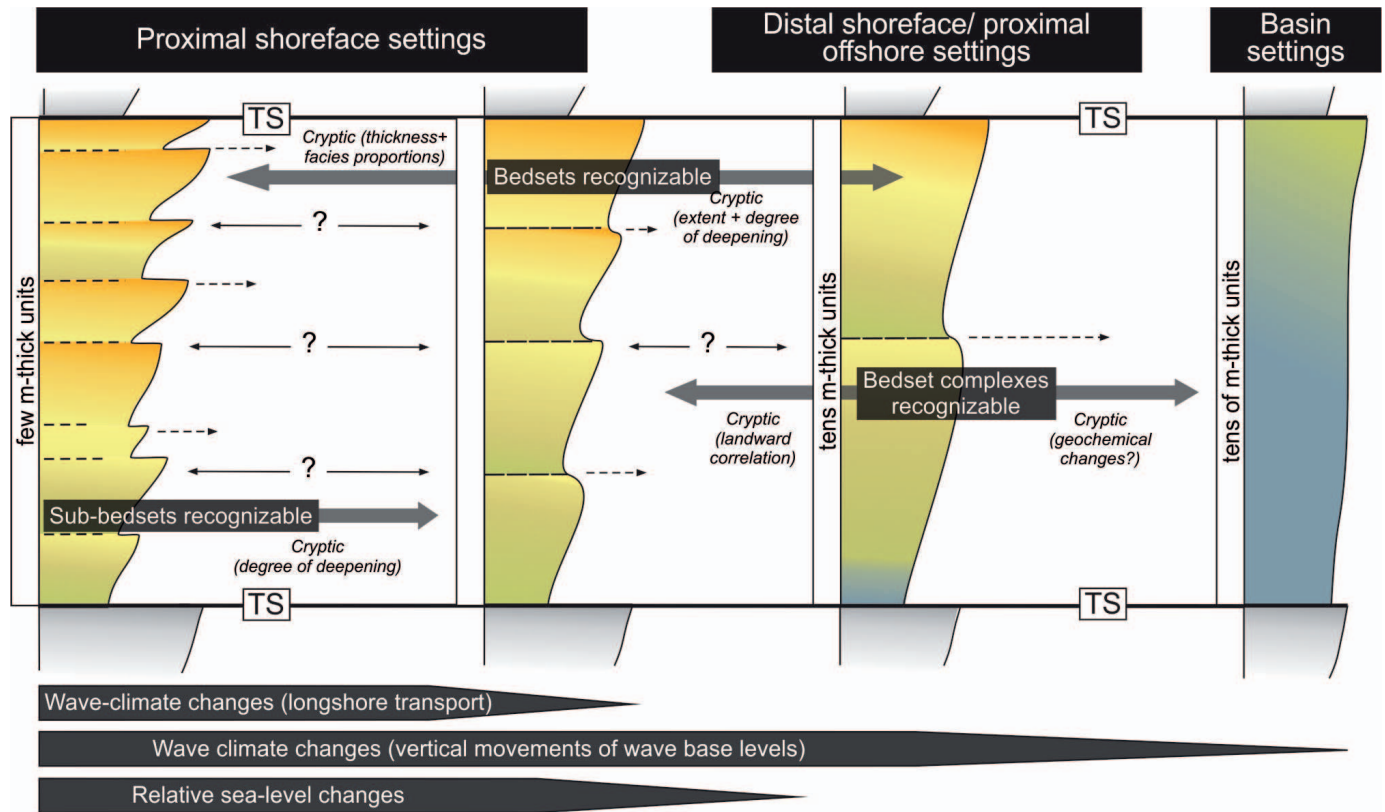
Fig. 14.—Conceptual framework showing intra-parasequence stratigraphic units and their lateral correlation in an idealized siliciclastic, shoreface–shelf parasequence, based on the Pilmatué Member case study. Some units become more cryptic (or apparent) depending on the proximal-to-distal location of the studied section. Bedset complexes are easily identifiable in intermediate-to-distal settings, and the landward correlation of boundaries allows their recognition in proximal settings. FWB, fair-weather base level; SWB, storm base level; LC, longshore currents.

Implications for the Definition of High-Frequency Stratigraphic Units in Ancient and Holocene Examples

About two decades ago, Hampson and Storms (2003) suggested that the intra-parasequence stratigraphy of shoreface–shelf systems was more complicated than what was reflected by the existing facies and sequence-stratigraphic models. Our results might be compared to other studies focusing on the high-resolution intra-parasequence stratigraphy of ancient and recent shallow-marine systems, as well as existing hierarchical frameworks (e.g., that proposed by Ainsworth et al. 2019). The sedimentologic and stratigraphic attributes used in the Pilmatué Member allow us to compare quantitative data between different high-resolution case studies. Bedset-thickness values in this study (Fig. 15A) are smaller than those in the widely studied Blackhawk Formation, Book Cliffs (Utah, USA), where average thickness values are around 13 m, ranging from 2 to 30 m (Fig. 15B; compiled and calculated from Pattison 1995; Hampson 2000; Hampson and Storms 2003; Storms and Hampson 2005; Sømme et al. 2008; Charvin et al. 2010; Hampson et al. 2011; Forzoni et al. 2015). The average thickness of the Book Cliffs bedsets is closer to that of bedset complexes in the present study (Fig. 13B). Bedset boundaries are commonly 1–6 km in lateral extent in the Book Cliffs examples (Hampson 2000; Sømme et al. 2008; Forzoni et al. 2015), but for up to 10 km in the Pilmatué Member (Fig. 15A). This relatively trivial difference could be related to the presence of shell-bed deposits in the Pilmatué Member, which in some cases allow for bounding surfaces to be traced in offshore settings. The degree of deepening of bedset boundaries in the Book Cliffs examples rarely exceeds a vertical shift of one facies association (DD1), whereas in the Pilmatué Member, equivalent boundaries can occasionally

exhibit a larger shift of two facies associations (DD2). The fact that bedsets defined in the Book Cliffs examples show clear overlapping in their attributes with both bedsets and bedset complexes of the Pilmatué Member suggests that some genetic units that have been defined as bedsets in the Book Cliffs could be revisited in the light of this new approach, to evaluate the chances of some of them representing higher or lower hierarchies as defined in this contribution. In this context, Onyenanu et al. (2018) suggested that in some already defined bedsets (sensu O'Byrne and Flint 1995) of the Grassy Member (Parasequence "G"), there were several smaller-scale, coarsening-upward units that could be attributed to the sub-bedset scale as proposed in this contribution. The bedset scale was not enough to honor the complex stratal architecture that exhibits the genetic units they studied in the Book Cliffs. The two bedsets studied by Onyenanu et al. (2018) can be confirmed as bedset from the point of view of thickness and facies proportion in the regressive interval and hence, their containing cojoined sandstone beds would correspond to sub-bedsets.

Shallowing-upward marine successions are also commonly documented in Holocene progradational coastal and deltaic systems and, in many cases, they are referred as parasequences (e.g., Amorosi et al. 1999, 2008). As the results emerging from the study of these better-age-constrained stratigraphic units are important for the understanding of forcing mechanisms, and those lessons can be extrapolated back to the ancient record, a fundamental question is: are these Holocene stratigraphic units size-equivalent to parasequences typically defined in ancient strata? A quantitative comparison between the Holocene deltaic shallowing-upward successions of the Po Plain (Adriatic coast, Italy) and the Pilmatué Member stratigraphic units suggests significant differences, as highlighted below.
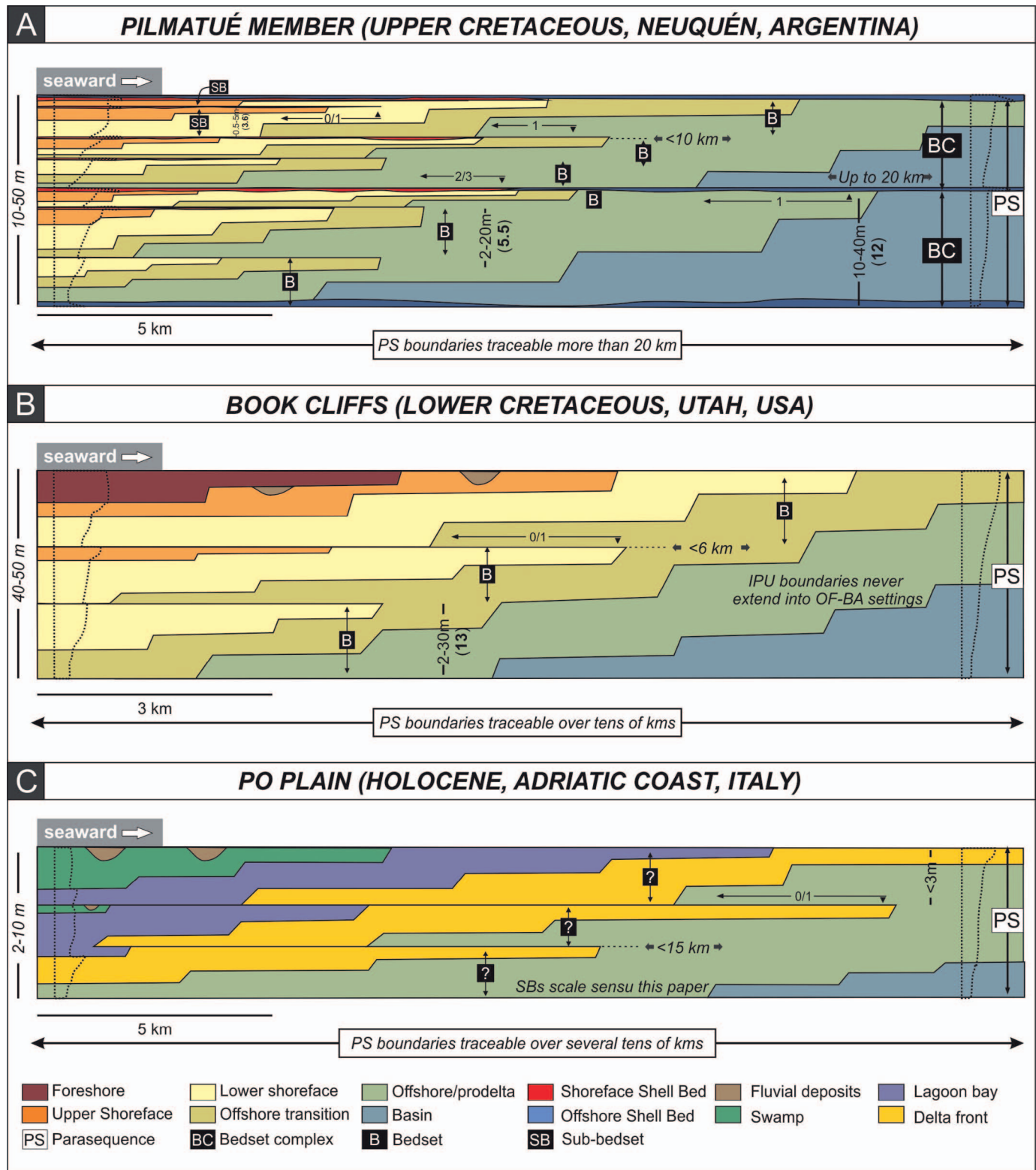
FIG. 15.—Comparison of the **A)** intra-parasequence hierarchy characterized for the Pilmatué Member in this study with the stratal architecture of **B)** Cretaceous (Book Cliffs), and **C)** Holocene (Po Plain) examples (Part B compiled from Pattison 1995; Hampson 2000; Hampson and Storms 2003; Storms and Hampson 2005; Sømme et al. 2008; Charvin et al. 2010; Hampson et al. 2011; Forzoni et al. 2015, and Part C from Amorosi et al. 2008, 2017; Bruno et al. 2017). The evaluation of sedimentologic and stratigraphic attributes shows some similarities and discrepancies between the three examples.

In the Po Plain, up to eight deltaic successions have been ascribed to parasequences (Fig. 15C) (Amorosi et al. 2017). The first outstanding difference in terms of objective quantitative attributes is that the thickness of those parasequences ranges from 2 to 10 m, which clearly falls in the thickness range of bedsets and sub-bedsets as defined here (Fig. 13A), and not on the scale of parasequences commonly defined both in the Pilmatué Member (Schwarz et al. 2018; this study) and in the Book Cliffs (e.g., Hampson et al. 2011). Additionally, the shallowing-upward smaller-scale units in the Po Plain parasequences are < 3 m thick (Fig. 15C), which would undoubtedly fall in our sub-bedset category. Moreover, when analyzing the degree of deepening across surfaces bounding the Po Plain parasequences, a value of DD0 to DD1 dominates over the study area (Fig. 15C). These degree-of-deepening values clearly depart from those measured in the Pilmatué Member parasequences (typically DD > 2) and are more similar to the attributes observed for the surfaces bounding bedsets. An additional difference is that minor, intra-parasequence bounding surfaces in the Po Plain examples have been recorded in the marine-to-nonmarine transition (lagoonal and swamp deposits representing backshore and/or interdistributary-plain settings), which does not occur in the Pilmatué Member examples.

The differences in the Pilmatué Member, Blackhawk Formation (Book Cliffs), and Po Plain examples can be analyzed from two different points of view. Variations could be related to the intrinsic characteristics of each depositional system and its corresponding basin. Po Plain deposits represent depositional conditions in a well-developed wave-dominated delta, whereas paleoenvironmental reconstructions for several parasequences in the Book Cliffs are interpreted to represent wave-dominated shoreface systems genetically associated with coastal-plain settings and, occasionally, incised fluvial valleys (Pattison 1995; Hampson et al. 2008, 2012; Forzoni et al. 2015). Unlike these examples, deposits of the Pilmatué Member should be compared to nondeltaic strandplains, i.e., those systems that do not exhibit nearby river input but are fed by long cells of littoral transport (Schwarz et al. 2018, 2021).

Another explanation could be that genetic units defined by using the same terminology should not be considered as equivalent. The available criteria suggest that parasequences from the Po Plain (Fig. 15C) are closer in terms of their attributes to those units defined as bedsets in the Pilmatué Member and Book Cliffs (Fig. 15A, B). Thus, independently of the term used to define the specific genetic unit, lessons concerning timespans and forcing mechanisms that operated over the evolution of Holocene parasequences should not be considered as suitable for ancient parasequences, but perhaps to smaller-scale hierarchical units. This has a significant impact when selecting modern analogs to apply to high-resolution, shallow-marine successions.

Ainsworth et al. (2019) proposed a hierarchical analysis made from comparing Holocene and ancient deltaic strandplains that could help to resolve the inconsistencies described above. This hierarchical analysis from vertical successions shows some possible equivalences in terms of stratigraphic attributes with the interpreted hierarchy of the Pilmatué Member (e.g., element set—sub-bedsets, element complex sets—bedsets or bedset complexes). However, to confirm possible equivalences, it would be necessary to analyze the lateral extents and three-dimensional configurations of hierarchical units, including in intermediate to distal settings.

CONCLUSIONS

This paper uses a set of standardized sedimentologic and stratigraphic attributes to characterize intra-parasequence genetic units in the Pilmatué Member, Neuquén Basin, Argentina. Six sedimentologic and stratigraphic attributes were quantified and compared from 42 intra-parasequence units recognized in 10 parasequences. These parameters involve the internal evolution of successive units (number of IPUs, thickness, and facies proportions in the regressive interval), as well as those related to the development of bounding surfaces (degree of deepening, lateral extent, and type and lateral extent of the thin transgressive deposits). By applying this approach to a 16-km-long proximal-to-distal outcrop transect, a hierarchical scheme of three different intra-parasequence genetic units was identified from larger to smaller units: bedset complexes, bedsets, and sub-bedsets.

Bedset complexes are stratigraphic units 10–40 m thick that represent the highest hierarchy of intra-parasequence stratigraphic units. They typically record a shallowing-upward succession from basin to upper-shoreface deposits, interrupted by surfaces 5 to 16 km long with a degree of deepening of one facies association at least along the 70% of their extent (with a maximum of three facies associations) and commonly associated with offshore shell beds. Bedsets are offshore to upper-shoreface successions, 2–20 m thick, bounded by surfaces up to 10 km long with a degree of deepening of zero to one at least along 70% of their extent, and that may be associated with shell beds (preferentially shoreface shell beds). Sub-bedsets are successions 0.5–5 m thick typically composed of lower- and upper-shoreface deposits (with subordinated offshore-transition facies), and frequently limited by surfaces 0.5 to 2 km long exhibiting a degree of deepening of zero to one for 80–100% of their extent, that may be associated with shoreface shell-bed deposits. The hierarchical analysis showed how the stacking of two or three genetic units commonly form the subsequent higher hierarchy from: 1) sub-bedsets, 2) bedsets, 3) bedset complexes, and 4) parasequences. Not all the criteria are equally effective for discriminating between these different categories, mostly due to the overlapping, and in any case a combination of two or more seems to be more recommended. Moreover, as the spatial sampling increases (e.g., observations in less than 0.5 km), smaller-scale units such as sub-bedsets can be confidentially defined.

The set of parameters related to bounding surfaces are chiefly better for discriminating between parasequences, bedset complexes, and bedsets, whereas the combination of IPU thickness with its proportion of facies associations in the regressive interval is useful to distinguish between bedsets and sub-bedsets. The proposed methodology needs to be tested by revisiting multiple cases of study concerning the intra-parasequence stratigraphy of shallow-marine environments. Preliminary comparisons with well-known examples have delineated some existing equivalences, but further work is required.

REFERENCES

AINSWORTH, R.B., VAKARELOV, B.K., MACEACHERN, J.A., RARITY, F., LANE, T.I., AND NANSON, R.A., 2017, Anatomy of a shoreline regression: implications for the high-resolution stratigraphic architecture of deltas: Journal of Sedimentary Research, v. 87, p. 425–459, doi:10.2110/jsr.2017.26.

AINSWORTH, R.B., VAKARELOV, B.K., EIDE, C.H., HOWELL, J.A., AND BOURGET, J., 2019, Linking the high-resolution architecture of modern and ancient wave-dominated deltas: processes, products, and forcing factors: Journal of Sedimentary Research, v. 89, p. 168–185, doi:10.2110/jsr.2019.7.

AMOROSI, A., COLALONGO, M.L., FUSCO, F., PASINI, G., AND FIORINI, F., 1999, Glacio-eustatic control of continental–shallow marine cyclicity from late Quaternary deposits of the southeastern Po Plain, northern Italy: Quaternary Research, v. 52, p. 1–13, doi: 10.1006/qres.1999.2049.

AMOROSI, A., DINELLI, E., ROSSI, V., VAIANI, S.C., AND SACCHETTO, M., 2008, Late Quaternary palaeoenvironmental evolution of the Adriatic coastal plain and the onset of Po River Delta: Palaeogeography, Palaeoclimatology, Palaeoecology, v. 268, p. 80–90, doi: 10.1016/j.palaeo.2008.07.009.

AMOROSI, A., BRUNO, L., CAMPO, B., MORELLI, A., ROSSI, V., SCARPONI, D., HONG, W., BOHACS, K.M., AND DREXLER, T.M., 2017, Global sea-level control on local parasequence architecture from the Holocene record of the Po Plain, Italy: Marine and Petroleum Geology, v. 87, p. 99–111, doi:10.1016/j.marpetgeo.2017.01.020.

BERTON, F., GUEDES, C.C.F., VESELY, F.F., SOUZA, M.C., ANGULO, R.J., ROSA, M.L.C.C., AND BARBOZA, E.G., 2018, Quaternary coastal plains as reservoir analogs: wave-dominated sand-body heterogeneity from outcrop and ground-penetrating radar, central Santos Basin, southeast Brazil: Sedimentary Geology, v. 379, p. 97–113, doi: 10.1016/j.sedgeo.2018.11.008.

BOHACS, K.M., LAZAR, O.R., AND DEMKO, T.M., 2014, Parasequence types in shelfal mudstone strata: quantitative observations of lithofacies and stacking patterns, and conceptual link to modern depositional regimes: Geology, v. 42, p. 131–134, doi:10.1130/G35089.1.

BRUNO, L., BOHACS, K.M., CAMPO, B., DREXLER, T.M., ROSSI, V., SAMMARTINO, I., SCARPONI, D., HONG, W., AND AMOROSI, A., 2017, Early Holocene transgressive palaeogeography in the Po coastal plain (northern Italy): Sedimentology, v. 64, p. 1792–1816, doi: 10.1111/sed.12374.

CAMPBELL, C.V., 1967, Lamina, laminaset, bed and bedset: Sedimentology, v. 8, p. 7–26, doi:10.1111/j.1365-3091.1967.tb01301.x.

CATTANEO, A., AND STEEL, R.J., 2003, Transgressive deposits: a review of their variability: Earth-Science Reviews, v. 62, p. 187–228, doi:10.1016/S0012-8252(02)00134-4.

CATUNEANU, O., 2019, Scale in sequence stratigraphy: Marine and Petroleum Geology, v. 106, p. 128–159, doi:10.1016/j.marpetgeo.2019.04.026.

CHARVIN, K., HAMPSON, G.J., GALLAGHER, K.L., AND LABOURDETTE, R., 2010, Intra-parasequence architecture of an interpreted asymmetrical wave-dominated delta: Sedimentology, v. 57, p. 760–785, doi:10.1111/j.1365-3091.2009.01118.x.

COLOMBERA, L., AND MOUNTNEY, N.P., 2020, On the geological significance of clastic parasequences: Earth-Science Reviews, v. 201, p. 103062, doi:10.1016/j.earscirev.2019.103062.

FORZONI, A., HAMPSON, G.J., AND STORMS, J.E.A., 2015, Along-strike variations in stratigraphic architecture of shallow-marine reservoir analogues: Upper Cretaceous Panther Tongue delta and coeval shoreface, Star Point Sandstone, Wasatch Plateau, Central Utah, USA: Journal of Sedimentary Research, v. 85, p. 968–989, doi:10.2110/jsr.2015.69.

HAMPSON, G.J., 2000, Discontinuity surfaces, clinoforms, and facies architecture in a wave-dominated, shoreface–shelf parasequence: Journal of Sedimentary Research, v. 70, p. 325–340, doi:10.1306/2DC40914-0E47-11D7-8643000102C1865D.

HAMPSON, G.J., AND STORMS, J.E.A., 2003, Geomorphological and sequence stratigraphic variability in wave-dominated, shoreface–shelf parasequences: Sedimentology, v. 50, p. 667–701, doi:10.1046/j.1365-3091.2003.00570.x.

HAMPSON, G.J., RODRIGUEZ, A.B., STORMS, J.E.A., JOHNSON, H.D., AND MEYER, C.T., 2008, Geomorphology and high-resolution stratigraphy of wave-dominated shoreline deposits: impact on reservoir-scale facies architecture, in Hampson, G.J., Steel, R.J., Burgess, P.M., and Dalrymple, R.W., eds., Recent Advances in Models of Siliciclastic Shallow-Marine Stratigraphy: SEPM, Special Publication 90, p. 117–142.

HAMPSON, G.J., GANI, M.R., SHARMAN, K.E., IRFAN, N., AND BRACKEN, B., 2011, Along-strike and down-dip variations in shallow-marine sequence stratigraphic architecture: Upper Cretaceous Star Point Sandstone, Wasatch Plateau, Central Utah, USA: Journal of Sedimentary Research, v. 81, p. 159–184, doi:10.2110/jsr.2011.15.

HAMPSON, G.J., GANI, M.R., SAHOO, H., RITTERSBACHER, A., IRFAN, N., RANSON, A., JEWELL, T.O., GANI, N.D., HOWELL, J.A., BUCKLEY, S.J., AND BRACKEN, B., 2012, Controls on large-scale patterns of fluvial sandbody distribution in alluvial to coastal plain strata: Upper Cretaceous Blackhawk Formation, Wasatch Plateau, Central Utah, USA: Sedimentology, v. 59, p. 2226–2258, doi: 10.1111/j.1365-3091.2012.01342.x.

HOWELL, J.A., SCHWARZ, E., SPALLETTI, L.A., AND VEIGA, G.D., 2005, The Neuquén Basin: an overview, in Veiga, G.D., Spalletti, L.A., Howell, J.A., and Schwarz, E., The Neuquén Basin, Argentina: A Case Study in Sequence Stratigraphy and Basin Dynamics: Geological Society of London, Special Publication 252, p. 1–14, doi:10.1144/GSL.SP.2005.252.01.01.

ISLA, M.F., SCHWARZ, E., AND VEIGA, G.D., 2018, Bedset characterization within a wave-dominated shallow-marine succession: an evolutionary model related to sediment imbalances: Sedimentary Geology, v. 374, p. 36–52, doi:10.1016/j.sedgeo.2018.07.003.

ISLA, M.F., CORONEL, M.D., SCHWARZ, E., AND VEIGA, G.D., 2020a, Depositional architecture of a wave-dominated clastic shoreline (Pilmatué Member, Argentina): improving knowledge about the stratigraphic record of bar–trough systems: Marine and Petroleum Geology, v. 118, no. 104417, doi:10.1016/j.marpetgeo.2020.104417.

ISLA, M.F., REMIREZ, M.N., SCHWARZ, E., AND VEIGA, G.D., 2020b, Vertical changes in shoreline morphology at intra-parasequence scale: Latin American Journal of Sedimentary and Basin Analysis, v. 27, p. 85–106.

ISLA, M.F., SCHWARZ, E., AND VEIGA, G.D., 2020c, Record of a nonbarred clastic shoreline: Geology, v. 48, p. 338–342, doi: 10.1130/G46800.1.

KAMOLA, D.L., AND VAN WAGONER, J.C., 1995, Stratigraphy and facies architecture of parasequences with examples from the Spring Canyon Member, Blackhawk Formation, Utah, in Bertram, G.T., ed., Sequence Stratigraphy of Foreland Basin Deposits: Outcrop and Subsurface Examples from the Cretaceous of North America: American Association of Petroleum Geologists, Memoir 64, p. 27–64.

LEGARRETA, L., AND ULIANA, M.A., 1991, Jurassic–Cretaceous marine oscillations and geometry of a back-arc basin fill, central Argentine Andes, in MacDonald, D.I.M., ed., Sedimentation, Tectonics and Eustacy: Sea-Level Changes at Active Margins:

International Association of Sedimentologist, Special Publication 12, p. 429–450, doi:10.1002/9781444303896.ch23

MITCHUM, R.M., JR., AND VAN WAGONER, J.C., 1991, High-frequency sequences and their stacking patterns: sequence-stratigraphic evidence of high-frequency eustatic cycles: Sedimentary Geology, v. 70, p. 131–160.

MOORE, S.A., BIRGENHEIER, L.P., GREB, M.D., MINISINI, D., TUNIK, M., AND OMARINI, J., 2020, Facies heterogeneity and source potential of carbonate–mudstone-dominated distal ramp deposits, Agrio Formation, Neuquén Basin, Argentina: Journal of Sedimentary Research, v. 90, p. 533–570, doi: 10.2110/jsr.2020.25.

O'BYRNE, C.J., AND FLINT, S., 1995, Sequence, parasequence, and intraparasequence architecture of the Grassy Member, Blackhawk Formation, Book Cliffs, Utah, U.S.A, in Van Wagoner, J.C., and Bertram, G.T., eds., Sequence Stratigraphy of Foreland Basin Deposits: Outcrop and Subsurface Examples from the Cretaceous of North America: American Association of Petroleum Geologists, Memoir 64, p. 225–255.

ONYENANU, G.I., JACQUEMYN, C.E.M.M., GRAHAM, G.H., HAMPSON, G.J., FITCH, P.J.R., AND JACKSON, M.D., 2018, Geometry, distribution and fill of erosional scours in a heterolithic distal lower shoreface sandstone reservoir analogue: Grassy Member, Blackhawk Formation, Book Cliffs, Utah, USA: Sedimentology, v. 65, p. 1731–1760, doi: 10.1111/sed.12444.

PATRUNO, S., HAMPSON, G.J., AND JACKSON, C.A., 2015, Quantitative characterisation of deltaic and subaqueous clinoforms: Earth-Science Reviews, v. 142, p. 79–119, doi: 10.1016/j.earscirev.2015.01.004.

PATTISON, S.A., 1995, Sequence stratigraphic significance of sharp-based lowstand shoreface deposits, Kenilworth Member, Book Cliffs, Utah: American Association of Petroleum Geologists, Bulletin, v. 79, p. 444–462, doi:10.1306/8D2B155C-171E-11D7-8645000102C1865D.

POSAMENTIER, H.W., AND ALLEN, G.P., 1999, Siliciclastic Sequence Stratigraphy: Concepts and Applications: SEPM, Concepts in Sedimentology and Paleontology 7, 210 p.

REMIREZ, M.N., SPALLETTI, L.A., AND ISLA, M.F., 2020, Petrographic, mineralogical and geochemical characterization of fine-grained rocks of the Pilmatué Member (Upper Valanginian–lower hauterivian) of the Neuquén Basin (Argentina): implications for siliciclastic input, carbonate productivity and redox conditions: Journal of South American Earth Sciences, v. 102, no. 102663, doi:10.1016/j.jsames.2020.102663.

SCHWARZ, E., AND HOWELL, J.A., 2005, Sedimentary evolution and depositional architecture of a Lowstand Sequence Set: Lower Cretaceous Mulichinco Formation, Neuquén Basin, Argentina, in Veiga, G.D., Spalletti, L.A., Howell, J., and Schwarz, E., eds., The Neuquén Basin, Argentina: A Case Study in Sequence Stratigraphy and Basin Dynamics: Geological Society of London, Special Publication 252, p. 109–138, doi:10.1144/GSL.SP.2005.252.01.06.

SCHWARZ, E., SPALLETTI, L.A., AND HOWELL, J.A., 2006, Sedimentary response to a tectonically-induced sea-level fall in a shallow back-arc basin: the Mulichinco Formation (Lower Cretaceous), Neuquén Basin, Argentina: Sedimentology, v. 53, p. 55–81, doi:10.1111/j.1365-3091.2005.00753.x.

SCHWARZ, E., SPALLETTI, L.A., VEIGA, G.D., AND FANNING, M., 2016a, First U-Pb SHRIMP Age for the Pilmatué Member (Agrio Formation) of the Neuquén Basin, Argentina: implications for the Hauterivian Lower Boundary: Cretaceous Research, v. 58, p. 223–233, doi:10.1016/j.cretres.2015.10.003.

SCHWARZ, E., VEIGA, G.D., TRENTINI, G.Á., AND SPALLETTI, L.A., 2016b, Climatically versus eustatically controlled, sediment-supply-driven cycles: carbonate–siliciclastic, high-frequency sequences in the Valanginian of the Neuquén Basin (Argentina): Journal of Sedimentary Research, v. 86, p. 312–335.

SCHWARZ, E., VEIGA, G.D., ÁLVAREZ TRENTINI, G., ISLA, M.F., AND SPALLETTI, L.A., 2018, Expanding the spectrum of shallow-marine, mixed carbonate–siliciclastic systems: processes, facies distribution, and depositional controls of a siliciclastic-dominated example: Sedimentology, v. 65, p. 1558–1589, doi:10.1111/sed.12438.

SCHWARZ, E., FINZEL, E.S., VEIGA, G.D., RAPELA, C.W., ECHEVARRIA, C., AND SPALLETTI, L.A., 2021, U-Pb geochronology and paleogeography of the Valanginian–Hauterivian Neuquén Basin: implications for Gondwana-scale source areas: Geosphere, v. 17, p. 244–270, doi: 10.1130/GES02284.1.

SØMME, T.O., HOWELL, J.A., HAMPSON, G.J., AND STORMS, 2008, Genesis, architecture, and numerical modeling of intra-parasequence discontinuity surfaces in wave-dominated deltaic deposits: Upper Cretaceous Sunnyside Member, Blackhawk Formation, Book Cliffs, Utah, USA, in Hampson, G.J., Steel, R.J., Burgess, P.M., and Dalrymple, R.W., eds., Recent Advances in Models of Siliciclastic Shallow-Marine Stratigraphy: SEPM, Special Publication 90, p. 421–441.

SPALLETTI, L.A., VEIGA, G.D., AND SCHWARZ, E., 2011, La Formación Agrio (Cretácico Temprano) en la Cuenca Neuquina, in Leanza, H., Vallés, J., Arregui, C., and Danieli, J.C., eds., Geología y Recursos Naturales de la Provincia del Neuquén: Buenos Aires, Relatorio del XVIII Congreso Geológico Argentino, p. 145–160.

STORMS, J.E.A., AND HAMPSON, G.J., 2005, Mechanisms for forming discontinuity surfaces within shoreface–shelf parasequences: sea level, sediment supply, or wave regime?: Journal of Sedimentary Research, v. 75, p. 67–81, doi:10.2110/jsr.2005.007.

VAN WAGONER, J.C., POSAMENTIER, H.W., MITCHUM, R.M., VAIL, P.R., SARG, J.F., LOUTIT, T.S., AND HARDENBOL, J., 1988, An overview of the fundamentals of sequence stratigraphy and key definitions, in Wilgus, C.K., Hastings, B.S., Kendall, C.G.St.C., Posamentier, H.W., Ross, C.A., and Van Wagoner, J.C., eds., Sea Level Changes: An Integrated Approach: SEPM, Special Publication 42, p. 39–46.

VAN WAGONER, J.C., MITCHUM, R.M., CAMPION, K.M., AND RAHMANIAN, V.D., 1990, Siliciclastic Sequence Stratigraphy in Well Logs, Cores, and Outcrop: Concepts for

High-Resolution Correlation of Time and Facies: American Association of Petroleum Geologists, Methods in Exploration Series 7, 255 p.

VEIGA, G.D., SPALLETTI, L.A., AND FLINT, S.S., 2007, Anatomy of a fluvial lowstand wedge: the Avilé Member of the Agrio Formation (Hauterivian) in central Neuquén Basin (northwest Neuquén province), Argentina, in Nichols, G., Williams, E., and Paola, C., eds., Sedimentary Processes, Environments and Basins, A Tribute to Peter Friend: International Association of Sedimentologists, Special Publication 38, p. 341–365.

ZAMORA VALCARCE, G., RAPALINI, A.E., AND SPAGNUOLO, C.M., 2007, Reactivación de estructuras cretácicas durante la deformación miocena, faja plegada del Agrio, Neuquén: Asociación Geológica Argentina, Revista, v. 62, p. 299–307.

ZECCHIN, M., AND CATUNEANU, O., 2013, High-resolution sequence stratigraphy of clastic shelves I: units and bounding surfaces: Marine and Petroleum Geology, v. 39, p. 1–25, doi:10.1016/j.marpetgeo.2012.08.015.

ZECCHIN, M., CAFFAU, M., CATUNEANU, O., AND LENAZ, D., 2017, Discrimination between wave-ravinement surfaces and bedset boundaries in Pliocene shallow-marine deposits, Crotone Basin, southern Italy: an integrated sedimentological, micropalaeontological and mineralogical approach: Sedimentology, v. 64, p. 1755–1791, doi:10.1111/sed.12373.

ZECCHIN, M., CATUNEANU, O., AND CAFFAU, M., 2019, Wave-ravinement surfaces: classification and key characteristics: Earth-Science Reviews, v. 188, p. 210–239, doi:10.1016/j.earscirev.2018.11.011.